

Surface states, Friedel oscillations, and spin accumulation in p -doped semiconductors

Tudor D. Stanescu and Victor Galitski

Department of Physics, University of Virginia, Charlottesville, VA 22904-4714

(Dated: August 23, 2018)

We consider a hole-doped semiconductor with a sharp boundary and study the boundary spin accumulation in response to a charge current. First, we solve exactly a single-particle quantum mechanics problem described by the isotropic Luttinger model in half-space and construct an orthonormal basis for the corresponding Hamiltonian. It is shown that the complete basis includes two types of eigenstates. The first class of states contains conventional incident and reflected waves, while the other class includes localized surface states. Second, we consider a many-body system in the presence of a charge current flowing parallel to the boundary. It is shown that the localized states contribute to spin accumulation near the surface. We also show that the spin density exhibits current-induced Friedel oscillations with three different periods determined by the Fermi momenta of the light and heavy holes. We find an exact asymptotic expression for the Friedel oscillations far from the boundary. We also calculate numerically the spin density profile and compute the total spin accumulation, which is defined as the integral of the spin density in the direction perpendicular to the boundary. The total spin accumulation is shown to fit very well the simple formula $S_{\text{tot}} \propto (1 - m_L/m_H)^2$, where m_L and m_H are the light- and heavy-hole masses. The effects of disorder are discussed. We estimate the spin relaxation time in the Luttinger model and argue that spin physics cannot be described within the diffusion approximation.

PACS numbers:

I. INTRODUCTION

Hole-doped semiconductors are a very well studied and industry developed class of materials. The fundamental description of these materials is usually based on effective models such as the Kane model or Luttinger model,¹ which capture most of the properties of a semiconductor. A key ingredient of these models is spin-orbit interaction, which couples the momentum with the orbital and spin degrees of freedom. It should be noted that the latter degrees of freedom in semiconductor systems attracted attention only very recently, when it was recognized that the spin-orbit coupling may lead to the possibility of spin control by electric means.^{2,3} On one hand, the predicted spin-charge coupling opens a possibility for new useful spintronics applications.^{4,5} On the other hand, it leads to a variety of new theoretical problems, which need to be clarified in order to understand the relevant experiments^{6,7,8}. The theoretical description of the intrinsic spin-Hall effect,^{3,9,10} which is one of the spin-charge coupling phenomena, relies on an elegant mathematical structure known as the Fermi surface Berry's phase.^{11,12,13} This structure originates from the spin-orbit splitting of the bands. Band crossings become sources of a fictitious magnetic field in momentum space, which leads to a non-trivial Berry's phase and may affect certain observables. In particular it leads to an anomalous contribution to the velocity operator. Consequently, any quantum mechanical operator, which involves the velocity acquires an anomalous contribution. An important example is the spin current operator (usually defined as a symmetrized product of the spin density and the velocity), which may acquire an anomalous component as well, if an electric current is present.^{3,14,15,16,17,18,19} The existence of the anomalous contribution to the spin current perpendicular to the electric current is an important prediction of the spin Hall effect theory. However, a direct experimental check of this prediction, while possible in principle, is not straightforward because the spin is not conserved, and as such, the spin current has no obvious physical meaning.^{20,21} Alternatively one can experimentally probe current-induced equilibrium spin density and that is what usually is measured in experiment. It is therefore desirable to develop a theory, which would allow one to calculate observables such as boundary spin accumulation directly and provide a clear understanding of the physical processes behind this effect. It is also desirable to search for other possible manifestations of the Fermi surface Berry's phase apart from the anomalous velocity.

In this paper we consider a three-dimensional hole-doped semiconductor described by the isotropic Luttinger model and in the presence of a boundary. We mostly discuss the clean limit when no impurities are present or, alternatively, a disordered system but only at small (ballistic) length-scales. We note here that the application of an electric field to a perfectly clean system would result in a non-equilibrium state and time-dependent spin density. To access equilibrium spin-Hall physics we assume that either the voltage drop occurs only in the contacts, or that there is a relaxation provided by impurities. In both cases there is an equilibrium charge current, which determines spin accumulation near the boundary.

Evaluation of the current-induced spin density involves solving the single-particle Schrödinger equation for the Luttinger Hamiltonian in a half-space. The corresponding solution contains a few important features, which are quite

different from the usual single-band quantum-mechanical problem. While the states of the bulk Luttinger model can be classified by quantum numbers corresponding to the double-degenerate heavy and light-hole bands, the boundary does not conserve these quantum numbers and mixes up different bands. For example, if a heavy-hole with positive chirality propagates towards the boundary in the direction close to normal, it gets reflected in all bands, which are heavy- and light-holes with positive and negative chiralities, and the reflected light holes have the angle of reflection (measured from the normal to the surface) larger than the angle of incidence. An important property of the solution is that for large enough angles of incidence, light holes are not reflected from the boundary at all, but instead get localized near the surface. These states are similar to the Tamm states,²² which appear in crystals due to an abrupt change of the electronic band structure at the boundary. We also point out that one can draw an intuitive analogy with optics by imagining that the heavy holes occupy a half-space with high index of refraction, while the light holes occupy the other half with a lower index of refraction. A wave propagating say from the medium with the high index of refraction (heavy hole) may get reflected from the interface (remains a heavy hole) or may get refracted and propagate in the other medium (becomes a light hole). For large enough angles of incidence, one expects total internal reflection, which is somewhat similar to the appearance of localized light-hole states in our language. It can be shown that these localized light-hole states contribute to spin accumulation if a current is present (below we study accumulation of the total orbital momentum, but occasionally call it “spin accumulation” for the sake of brevity).

To qualitatively understand the physics of the boundary spin accumulation in a many-particle system it is useful to recall the well-known problem of a free Fermi gas in the presence of a boundary. The boundary (or any other perturbation for this matter) leads to the Friedel oscillations in the particle density with the period of two Fermi momenta. We note that the integral of the density over distance reduces to the bulk density, *i.e.*, there is no boundary charge accumulation since the latter is conserved. A similar oscillatory behavior of the spin density may occur in spin-orbit coupled systems (*e.g.*, described by the Luttinger model) if a current is present. There are, however, two important differences: (i) The existence of multiple periods of Friedel oscillations (or beatings) due to two distinct Fermi momenta corresponding to the light and heavy holes; (ii) The non-zero integral of the spin density due to the non-conservation of spin. Summarizing the above qualitative discussion, we argue that non-zero spin density, which appears near the boundary in response to an applied current can be viewed as current-induced Friedel oscillations with non-zero spin accumulation originating from the localized (Tamm-like) surface states.

Our paper is structured as follows: In Sec. II we solve the quantum-mechanical problem of a particle described by the Luttinger Hamiltonian in a half-space. We show that for the angles of incidence greater than a critical angle θ_c , the eigenstates contain modes that are localized in the direction normal to the boundary. We construct a full orthonormal basis for the problem. Even though the formulation of the problem is very straightforward, its solution is technically challenging due to a cumbersome matrix structure of the Hamiltonian. Subsections II A and II B are devoted to a formal proof that certain symmetrized combinations of incident and reflected waves constitute a full orthonormal basis for the Hamiltonian. A reader not interested in the formal proof should skip to Sec. III.

In Sec. III we address the question of boundary spin accumulation in response to an external current. Using the orthonormal basis constructed in Sec. II, we obtain numerically the spin density profile near the boundary for various values of the ratio of the light and heavy hole masses, $\xi = m_L/m_H$. We also extract analytically the large-distance asymptotic behavior of the spin density, which is shown to oscillate with three distinct periods $2k_F^{(H)}$, $2k_F^{(L)}$, and $k_F^{(H)} + k_F^{(L)}$ (where $k_F^{(H)}$ and $k_F^{(L)}$ are Fermi momenta of the heavy and light holes correspondingly) and decay away from the boundary as a power law, $\propto 1/r^2$. In subsection III B, we define a quantity, which we call spin accumulation, by integrating the spin density over distance in the direction perpendicular to the boundary. We obtain the spin accumulation numerically and show that the total spin accumulation fits the simple formula $S_{\text{tot}} \propto (1 - \xi)^2$.

In Sec. IV, we discuss qualitatively the effects of disorder on the current-induced Friedel oscillations. Using the analogy between the spin accumulation effect and the usual Friedel (or RKKY) oscillations in disordered metals, we argue that one should expect an interesting behavior of the current-induced Friedel oscillations in the spin density in a disordered system. We argue that while the system-wide average value of the boundary spin density decays exponentially away from the boundary as $e^{-r/l}$ (where l is the mean free path), the higher moments and the *typical* spin density still decays as a power law r^{-2} . However, the latter has a random sign and the spin accumulation (*i.e.*, spin density averaged over large enough distances) decays exponentially as e^{-r/L_s} (where L_s is a spin relaxation length). We calculate the spin relaxation time and show that for all reasonable values of the spin-orbit coupling, the spin relaxation time is very short and has a universal value $\tau_s = 3\tau/2$. This short spin relaxation time implies that the spin relaxation length is of the order of the mean free path and, therefore, the hydrodynamic diffusion approximation does not apply for the Luttinger model.

II. EIGENSTATES FOR THE LUTTINGER HAMILTONIAN IN HALF-SPACE

The physics of a hole-doped semiconductor with diamond or zinc-blende structure is often described by the effective Luttinger Hamiltonian¹:

$$\hat{\mathcal{H}}_{\text{Lut}} = \frac{1}{2m} \left[\left(1 + \frac{5}{2}\gamma \right) \mathbf{k}^2 - 2\gamma(\mathbf{k} \cdot \hat{\mathbf{S}})^2 \right], \quad (1)$$

where m is the effective mass, $\mathbf{k} = (k_x, k_y, k_z)$ is the momentum and $\hat{\mathbf{S}} = (\hat{S}_x, \hat{S}_y, \hat{S}_z)$ represents the total angular momentum $3/2$ of the atomic orbital, i.e. the sum of the orbital angular momentum and the spin. The total angular momentum can be represented by three 4×4 matrices with explicit expressions given in Appendix A. For simplicity, we consider the spherically symmetric model described by one Luttinger parameter¹, γ , and we choose the units so that $\hbar = 1$.

For a system with translational symmetry, the Hamiltonian (1) can be diagonalized in a basis in which the helicity operator $\lambda = \mathbf{k} \cdot \hat{\mathbf{S}}/k$ is also diagonal. For a given wave vector \mathbf{k} , $\hat{\mathcal{H}}_{\text{Lut}}$ has two double degenerate eigenvalues

$$\begin{aligned} \epsilon_H(\mathbf{k}) &= \frac{1 - 2\gamma}{2m} k^2 \equiv \frac{k^2}{2m_H} & \text{for } \lambda = \pm \frac{3}{2}, \\ \epsilon_L(\mathbf{k}) &= \frac{1 + 2\gamma}{2m} k^2 \equiv \frac{k^2}{2m_L} & \text{for } \lambda = \pm \frac{1}{2}. \end{aligned} \quad (2)$$

These two bands are referred to as heavy-holes and light-holes, respectively. The corresponding eigenfunctions can be expressed in terms of a four-component spinor,

$$\Phi_{\mathbf{k}\lambda}(\mathbf{r}) = \frac{1}{\sqrt{\Omega}} e^{i\mathbf{k}\mathbf{r}} U_{\lambda}(\mathbf{n}_{\mathbf{k}}), \quad (3)$$

where Ω is the volume of the system, the label λ is $(\pm 3/2) \equiv (H\pm)$ for the heavy-holes and $(\pm 1/2) \equiv (L\pm)$ for the light-holes, and the spinors $U_{\lambda}(\mathbf{n}_{\mathbf{k}})$ depend on the orientation of the wave vector, $\mathbf{n}_{\mathbf{k}} = \mathbf{k}/|\mathbf{k}|$. Their explicit forms are given in Appendix A.

Next we consider a similar problem for a system defined in half-space, i.e. in the presence of a sharp boundary in the z direction defined by the potential

$$V(\mathbf{r}) = \begin{cases} 0 & \text{if } z > 0 \\ \infty & \text{if } z < 0 \end{cases} \quad (4)$$

Solving the quantum problem described by the Luttinger Hamiltonian (1) in the presence of the boundary is still a straightforward exercise. However, finding an orthonormal basis for this system, represents a technical challenge because of two main reasons: 1) The new eigenstates are, in general, linear combinations of bulk eigenfunctions $\Phi_{\mathbf{k}\lambda}(\mathbf{r})$ and are not automatically orthogonal on each other, and 2) The proper counting of modes is difficult, as the standard technique of imposing periodic boundary conditions and discretizing the momentum is not immediately applicable for eigenstates involving combinations of heavy and light holes. In this Section, we will direct our effort toward solving these difficulties with the goal of constructing an orthonormal basis for the Luttinger Hamiltonian in a half space. Let us notice that while k_x and k_y are still good quantum numbers for the full Hamiltonian $\hat{\mathcal{H}} = \hat{\mathcal{H}}_{\text{Lut}} + V(\mathbf{r})$, k_z and the helicity λ are not. The wave functions have to vanish at the boundary, i.e. for $z = 0$, while for positive values of z they are superpositions of incident and reflected waves. Let us consider the case of a $\lambda = +3/2$ incident heavy-hole (see Fig. 1). We can always choose the coordinate system so that $k_y = 0$ and $k_x \geq 0$ by properly rotating the axes. The full wave function corresponding to the reflection process represented schematically in Fig. 1 has the following form for positive values of z ,

$$\begin{aligned} \psi_{\mathbf{k}}^{(H+)}(\mathbf{r}) &= \frac{e^{ik_x x}}{\sqrt{C}} \left\{ U_{H+}(\theta) e^{ik_z z} + A_1 U_{H+}(\pi - \theta) e^{-ik_z z} + A_2 U_{H-}(\pi - \theta) e^{-ik_z z} \right. \\ &\quad \left. + B_1 U_{L+}(\pi - \phi) e^{iq_z z} + B_2 U_{L-}(\pi - \phi) e^{iq_z z} \right\}, \end{aligned} \quad (5)$$

where C is a normalization factor. All the reflection coefficients $A_i(\theta)$ and $B_i(\theta)$ are in general non-zero and are determined by the boundary condition $\psi_{\mathbf{k}}(z = 0) = 0$. The parameters that describe the reflected waves can be determined from the parameters of the incident wave using the momentum and energy conservation laws. Explicitly we have for the heavy-holes

$$\begin{cases} k'_x = k_x; \\ k'_y = k_y \equiv 0; \\ k'_z = -k_z; \end{cases} \quad \rightarrow \quad \theta' = \pi - \theta, \quad (6)$$

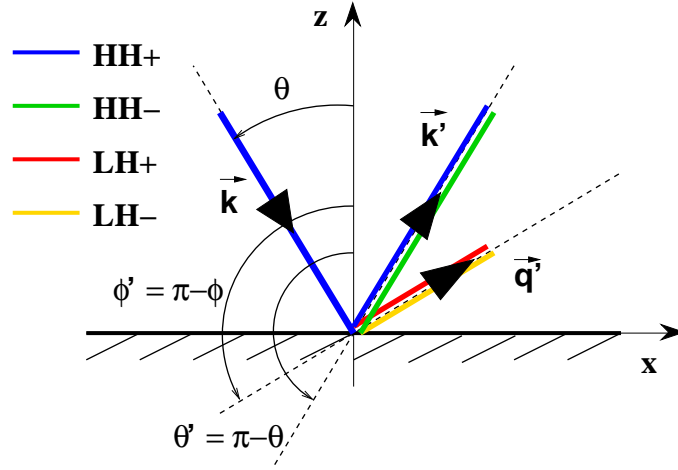


FIG. 1: (Color online) Scattering of an incident heavy-hole plane wave. By convention, the coordinate system is chosen so that $k_y = 0$ and $k_x \geq 0$. The angles θ , θ' and φ that describe the direction of propagation for a given wave are defined as the angles between the z -axis and $-\mathbf{p}$, where $\mathbf{p} \in \{\mathbf{k}, \mathbf{k}', \mathbf{q}'\}$, and belong to the interval $[0, \pi]$. The regime represented here corresponds to $\theta < \theta_c$ (see text) and the incident and reflected waves are described by the wave-functions defined by Eq. (3).

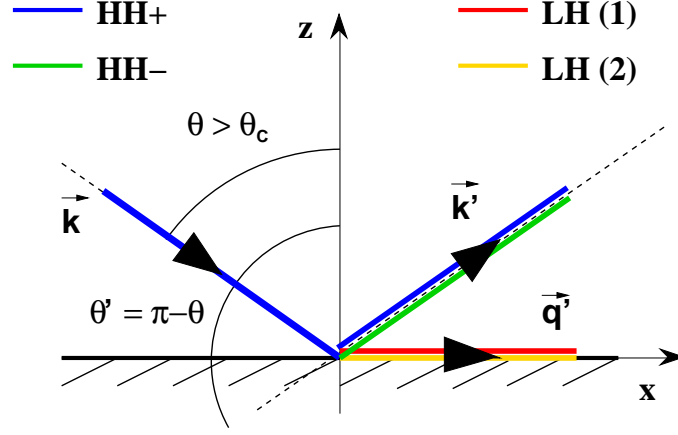


FIG. 2: (Color online) Scattering of an incident heavy-hole plane wave with the incident angle $\theta > \theta_c$. The reflected light-holes propagate parallel to the boundary and are localized in the z -direction. The wave function describing the reflection process is given by Eq. (9). Notice that the localized modes are described by two independent spinors $V_1(\chi)$ and $V_2(\chi)$ (see Appendix A).

where $\theta = \arccos(-k_z/k) \in [0, \pi/2]$ is the angle of the incident heavy-hole. Similarly we obtain for the light-holes

$$\begin{cases} q'_x = k_x; \\ q'_y = k_y \equiv 0; \\ q'_z = k[\xi - \sin^2(\theta)]^{1/2}; \end{cases} \quad \rightarrow \quad \phi' = \pi - \phi = \pi - \arccos\left(\sqrt{1 - \frac{\sin^2(\theta)}{\xi}}\right), \quad (7)$$

where $\xi = m_L/m_H \equiv (1 - 2\gamma)/(1 + 2\gamma)$ is the ratio between the light-hole and heavy-hole masses. Consequently, the wave function (5) is an eigenfunction of the full Hamiltonian with an eigenvalue $\epsilon_{\mathbf{k}} = k^2/2m_H = q^2/2m_L$. This solution exists as long as q_z is a real number, i.e. for incident angles smaller than the critical angle

$$\theta_c = \arcsin(\sqrt{\xi}). \quad (8)$$

For $\theta > \theta_c$ there are no light-holes propagating in the z -direction but, instead, the scattering problem has solutions that are localized at the boundary. This situation is illustrated schematically in Fig. 2. The localized modes are characterized by an imaginary wave vector $q_z = iQ$ and the corresponding wave function becomes

$$\psi_{\mathbf{k}}^{(H+)}(\mathbf{r}) = \frac{e^{ik_x x}}{\sqrt{C}} \{ U_{H+}(\theta) e^{ik_z z} + A_1 U_{H+}(\pi - \theta) e^{-ik_z z} + A_2 U_{H-}(\pi - \theta) e^{-ik_z z} \}$$

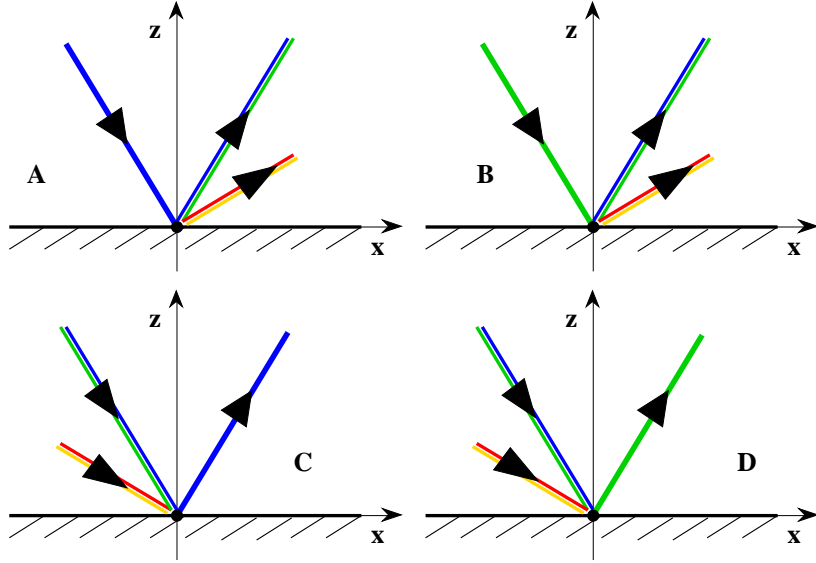


FIG. 3: (Color online) Family of reflection processes characterized by a given pair of reflection angles $(\theta, \phi(\theta))$. The color code is the same as in Fig. 1. Panel A represents schematically the same event as Fig. 1, the scattering of a heavy-hole with helicity $\lambda = +3/2$, while panel B represents the scattering of an incident heavy-hole with opposite helicity, $\lambda = -3/2$. Panels C and D illustrate “re-combination” processes where superpositions of heavy-holes and light-holes are reflected into a single heavy-hole mode with helicity $+3/2$ and $-3/2$, respectively. For incident heavy-hole angles $\theta > \theta_c$, the light-holes propagate parallel to the boundary ($\phi = \pi/2$), while they are localized in the z -direction, and are described by the spinors $V_i(\chi)$ given by Eq. (A3).

$$+ B_1 V_1(\chi) e^{-Qz} + B_2 V_2(\chi) e^{-Qz} \}, \quad (9)$$

where $V_i(\chi)$ are spinors describing the evanescent modes and the reflection coefficients are determined, as before, by the boundary condition. Explicit expressions for the $V_i(\chi)$ spinors are given in Appendix A. The angle χ and the wave vector that characterize the localized states are determined again using the conservations laws and we have

$$\begin{cases} q'_x = k_x; \\ q'_y = k_y \equiv 0; \\ q'_z \equiv iQ = ik[\sin^2(\theta) - \xi]^{1/2}; \end{cases} \quad \rightarrow \quad \chi = \arccos\left(\frac{\sqrt{\xi}}{\sin(\theta)}\right), \quad (10)$$

Notice that all the modes contained in the superpositions that define the wave-function in Eq. (5) and Eq. (9) are eigenfunctions of the Luttinger Hamiltonian corresponding to the same eigenvalue,

$$\begin{aligned} \hat{\mathcal{H}}_{\text{Lut}} [U_{H\pm}(\theta) e^{i\mathbf{k}\mathbf{r}}] &= \epsilon_k [U_{H\pm}(\theta) e^{i\mathbf{k}\mathbf{r}}], & \hat{\mathcal{H}}_{\text{Lut}} [U_{L\pm}(\phi) e^{i(k_x x + q_z z)}] &= \epsilon_k [U_{L\pm}(\phi) e^{i(k_x x + q_z z)}], \\ \hat{\mathcal{H}}_{\text{Lut}} [V_i(\phi) e^{i k_x x - Qz}] &= \epsilon_k [V_i(\phi) e^{i k_x x - Qz}], \end{aligned} \quad (11)$$

where

$$\epsilon_k = \frac{k_x^2 + k_z^2}{2m_H} = \begin{cases} \frac{k_x^2 + q_z^2}{2m_L}, & \text{if } \theta < \theta_c, \\ \frac{k_x^2 - Q^2}{2m_L}, & \text{if } \theta > \theta_c. \end{cases} \quad (12)$$

Also notice that all the scattering angles and the wave vectors can be expressed uniquely in terms of θ and $k = (k_x^2 + k_y^2 + k_z^2)^{1/2}$. In addition, the scattering coefficients A_i and B_i in Eq. (5) and Eq. (9) are functions of the angle θ of the incident heavy-hole. Their explicit form is given in Appendix B.

The wave function (5) is not the only eigenstate of the Hamiltonian $\hat{\mathcal{H}} = \hat{\mathcal{H}}_{\text{Lut}} + V(\mathbf{r})$ with the eigenvalue $\epsilon_k = k^2/2m_H$ that can be expressed as a superposition of propagating modes characterized by the scattering angles $(\theta, \phi(\theta))$. For example, a similar state can be obtained by starting with an incident heavy-hole with helicity $\lambda = -3/2$, (HH-). Moreover, we can imagine “re-combination” events, such as those represented schematically in Fig. 3 (panels C and D), or the corresponding scattering processes of light-holes shown in Fig. 4. From this family of states one

can extract sets of four linearly independent eigenfunctions, while all the others states can be expressed as linear combinations of these vectors. Our task is to identify such a complete set of orthogonal wave functions that would allow us to construct an orthonormal basis for the full quantum problem. The basic idea is to construct this set by taking certain symmetric linear combinations of the eigenfunctions represented in Fig. 3. The general expression for such a symmetrized eigenstate is

$$\begin{aligned} \Psi_{\mathbf{k}}^{\alpha}(\mathbf{r}) = & \frac{1}{\sqrt{\Omega}} e^{ik_x x} \{ [c_1^{\alpha} U_{H+}(\theta) + c_2^{\alpha} U_{H-}(\theta)] e^{ik_z z} + [c_3^{\alpha} U_{L+}(\phi) + c_4^{\alpha} U_{L-}(\phi)] e^{iq_z z} \\ & + [c_5^{\alpha} U_{H+}(\pi - \theta) + c_6^{\alpha} U_{H-}(\pi - \theta)] e^{-ik_z z} + [c_7^{\alpha} U_{L+}(\pi - \phi) + c_8^{\alpha} U_{L-}(\pi - \phi)] e^{-iq_z z} \}, \end{aligned} \quad (13)$$

where $|c_i^{\alpha}|^2 = |c_{i+4}^{\alpha}|^2$, $i \in \{1, 2, 3, 4\}$, i.e. the weight of each mode is the same for both the incident and the reflected waves. In constructing the symmetrized eigenfunctions, we use the fact that the reflection coefficients for the family of states described in Fig. 3 can be expressed in terms of the reflection coefficients of the state $\psi^{(H+)} \equiv \psi^A$ given by Eq. (B1). We write the corresponding wave-functions in the most general form given by Eq. (13). For example, the wave-function $\psi_{\mathbf{k}}^A$, corresponding to the process represented in Fig. 3A, will have the coefficients $c_1^A = 1$, $c_2^A = c_3^A = c_4^A = 0$, $c_5^A = A_1$, etc., up to an overall normalization factor that we omit. In Table I we summarize the relations between the coefficients of the wave-functions corresponding to the reflection processes represented in Fig. 3, omitting an overall normalization factor.

	c_1^{α}	c_2^{α}	c_3^{α}	c_4^{α}	c_5^{α}	c_6^{α}	c_7^{α}	c_8^{α}
ψ^A	1	0	0	0	A_1	A_2	B_1	B_2
ψ^B	0	1	0	0	$-A_2$	A_1	B_2	$-B_1$
ψ^C	A_1	$-A_2$	$-B_1$	B_2	1	0	0	0
ψ^D	A_2	A_1	B_2	B_1	0	1	0	0

TABLE I: Coefficients for the family of wave-functions represented in Fig. 3. The wave functions are expressed in the general form given by Eq. (13). The coefficients corresponding to the reflections from panels B, C and D (see Fig. 3) are expressed in terms of the coefficients for the process A which are given explicitly by Eq. (B1).

Next we introduce two pairs of symmetrized states defined as

$$\begin{aligned} \Psi_{\mathbf{k}}^{1\pm}(\mathbf{r}) &= \frac{1}{\sqrt{1+a^2}} \left[\left(1 - \frac{ab}{\sqrt{1-b^2}} \right) \psi^{AC\pm} + \frac{a}{\sqrt{1-b^2}} \psi^{BD\mp} \right], \\ \Psi_{\mathbf{k}}^{2\pm}(\mathbf{r}) &= \frac{1}{\sqrt{1+a^2}} \left[\left(a + \frac{b}{\sqrt{1-b^2}} \right) \psi^{AC\pm} - \frac{1}{\sqrt{1-b^2}} \psi^{BD\mp} \right], \end{aligned} \quad (14)$$

where $\psi^{AC\pm} = 1/\sqrt{N}(\psi^A \pm \psi^C)$ and $\psi^{BD\mp} = 1/\sqrt{N'}(\psi^B \mp \psi^D)$, with N and N' being normalization factors that insure $\langle \psi^{\alpha} | \psi^{\alpha} \rangle = 1$ for both linear combinations. The parameter 'b' is set equal to the scalar product of the two sets of linear combinations, $b = \langle \psi^{AC\pm} | \psi^{BD\mp} \rangle$, insuring the orthonormality of the eigenstates,

$$\langle \Psi^{i+} | \Psi^{j+} \rangle = \delta_{ij}, \quad \langle \Psi^{i-} | \Psi^{j-} \rangle = \delta_{ij}, \quad (15)$$

where δ_{ij} is the Kronecker δ -symbol. By varying the parameter 'a' we can change the weight of the heavy-hole and light-hole modes that contribute to a particular eigenfunction. For a state given by Eq. (13) the weight of the heavy-holes is defined as

$$W_{HH}^{\alpha} = |c_1^{\alpha}|^2 + |c_2^{\alpha}|^2 + |c_5^{\alpha}|^2 + |c_6^{\alpha}|^2, \quad (16)$$

while for the light-holes we have $W_{LH}^{\alpha} = 1 - W_{HH}^{\alpha}$. We choose the parameter 'a' to maximize the weight of the heavy-holes in the eigenstates $\Psi^{1\pm}$ and the weight of the light-holes in $\Psi^{2\pm}$. The convenience of this choice will become clear once we address the problem of counting the eigenstates. The explicit value of the parameter 'a' satisfying this condition is

$$a = \frac{1}{2W'} \left(W_{HH}^{BD\mp} - W_{HH}^{AC\pm} + \sqrt{(W_{HH}^{BD\mp} - W_{HH}^{AC\pm})^2 + 4(W')^2} \right), \quad (17)$$

where $W' = c_1^{AC\pm} c_1^{BD\mp} + c_2^{AC\pm} c_2^{BD\mp} + c_5^{AC\pm} c_5^{BD\mp} + c_6^{AC\pm} c_6^{BD\mp}$. Notice that, while in general the eigenstates $\Psi^{i\pm}$ represent a superposition of both heavy-hole and light-hole modes, in the particular case of normal incidence, $\theta = 0$,

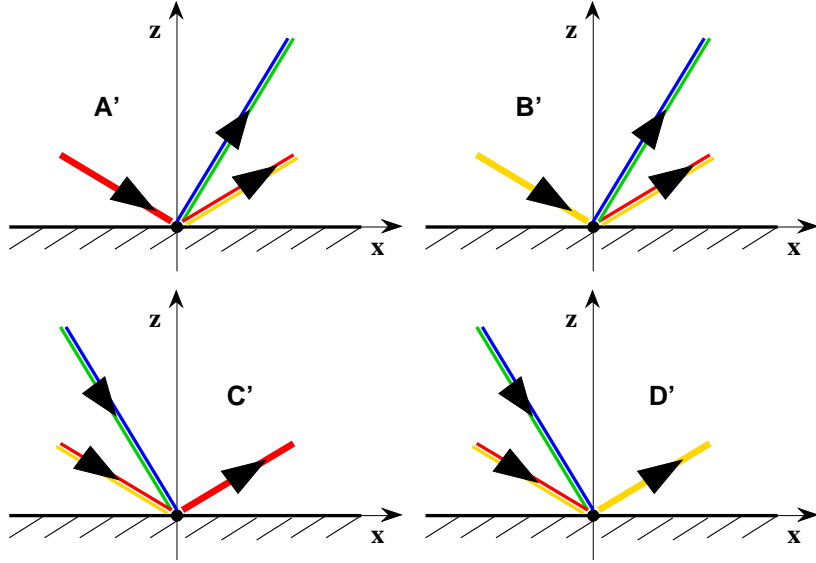


FIG. 4: (Color online) Light-hole reflections that belong to the same family as the processes represented schematically in Fig. 3. These reflections involve a single incident (panels A' and B') or reflected (panels C' and D') light-hole mode. The corresponding wave-functions can be written as linear combinations of wave-functions describing the heavy-hole scattering processes represented in Fig. 3. Same color code as in Fig. 1: blue - (HH+), green - (HH-), red - (LH+), yellow - (LH-).

	c_1^α	c_2^α	c_3^α	c_4^α	c_5^α	c_6^α	c_7^α	c_8^α
Ψ^{1+}	c_1^1	c_2^1	c_3^1	c_4^1	c_1^1	$-c_2^1$	$-c_3^1$	c_4^1
Ψ^{1-}	$-c_2^1$	c_1^1	c_4^1	$-c_3^1$	c_2^1	c_1^1	c_4^1	c_3^1
Ψ^{2+}	c_1^2	c_2^2	c_3^2	c_4^2	c_1^2	$-c_2^2$	$-c_3^2$	c_4^2
Ψ^{2-}	$-c_2^2$	c_1^2	c_4^2	$-c_3^2$	c_2^2	c_1^2	c_4^2	c_3^2

TABLE II: Relations between the coefficients of the symmetric eigenstates for an incident angle for the heavy-holes $\theta < \theta_c$. The wave functions for the pairs of states $\Psi_k^{1(2)+}$ and $\Psi_k^{1(2)-}$ (see Eq. (14)) are written in the general form given by Eq. (13). The existence of two pairs of modes labeled by 1 and 2 is reminiscent of the heavy- and light-holes of the bulk, while the degree of freedom labeled by '+' and '-' is the analogous of helicity. Notice that all the coefficients can be expressed in terms of two sets of four parameters, one set for each pair of modes $\alpha = 1\pm$ and $\alpha = 2\pm$, respectively.

$\Psi^{1\pm}$ contains only heavy-holes and $\Psi^{2\pm}$ contains only light-holes. In addition, for $\theta = \theta_c$, $\Psi^{2\pm}$ reduces again to a superposition of light-holes propagating parallel to the boundary, *i.e.*, $\phi(\theta_c) = \pi/2$. There is a symmetry between the modes contributing to Ψ^{i+} and the states with opposite helicity contributing to Ψ^{i-} . This symmetry translates into a set of relation between the corresponding coefficients that is summarized in Table II.

So far we have addressed the problem of finding a set of symmetric eigenstates in the case when the incident angle for the heavy-holes is smaller than the critical angle, $\theta < \theta_c$. Let us focus now on the case $\theta > \theta_c$, when the light-holes are localized near the boundary. There are two main differences between the two cases. The first one concerns the number of linearly independent eigenstates. Far from the boundary, the system should be locally equivalent to an infinite system and, consequently, the number of degrees of freedom should be the same. The set of four independent eigenstates that we obtained for $\theta < \theta_c$ corresponds to the double degenerate heavy-holes and light-holes of the infinite system. In contrast, for $\theta > \theta_c$ only the heavy-holes modes propagate in the z-direction and, therefore, we expect to have only two independent eigenfunction for a given incident angle. The second difference is a formal one and consist in the spinors $V_i(\chi)$ being complex, in contrast with U_λ which are real. Consequently, the coefficients of the eigenstates involving localized modes will be complex numbers. The coefficients A_i, B_i for the wave function (9) are given explicitly in appendix B. The symmetric eigenstates can be written again as superposition of reflection processes analogous to those in Fig. 3, except that this time the light-holes are localized modes confined near the boundary. The most general form of such an eigenstate can be written as

$$\Psi_{\mathbf{k}}^\alpha(\mathbf{r}) = \frac{1}{\sqrt{\Omega}} e^{ik_x x} \{ [c_1^\alpha U_{H+}(\theta) + c_2^\alpha U_{H-}(\theta)] e^{ik_z z} + [c_3^\alpha V_1(\chi) + c_4^\alpha V_2(\chi)] e^{-Qz} \} \quad (18)$$

$$+ [c_5^\alpha U_{H+}(\pi - \theta) + c_6^\alpha U_{H-}(\pi - \theta)] e^{-ik_z z} \},$$

where $Q(k, \theta)$ and $\chi(\theta)$ are given by Eq. (10). Again, the coefficients corresponding to a family of reflection processes similar to that represented in Fig. 3 are not all independent and we summarize the relations between them in Table III.

	c_1^α	c_2^α	c_3^α	c_4^α	c_5^α	c_6^α
ψ^A	1	0	B_1	B_2	A_1	A_2
ψ^B	0	1	iB_1	$-iB_2$	$-A_2$	A_1
ψ^C	A_1^*	$-A_2^*$	iB_1^*	iB_2^*	1	0
ψ^D	A_2^*	A_1^*	$-B_1^*$	B_2^*	0	1

TABLE III: Coefficients for a family of wave-functions with localized light-hole modes analogous to the scattering processes represented in Fig. 3. The wave functions are expressed in the general form given by Eq. (18). The complex coefficients corresponding to the reflection of a heavy-hole with helicity $-3/2$ (analog to the process represented in Fig. 3 panel B), as well as the “re-combination” processes (see Fig. 3 panels C and D), are expressed in terms of the coefficients for the heavy-hole $+3/2$ reflection (panel A) given by Eq. (B2).

Finally, we define the symmetrized eigenstates

$$\begin{aligned} \Psi_{\mathbf{k}}^1(\mathbf{r}) &= \frac{1}{\sqrt{C_1}} [\psi^{AC+} + i\psi^{BD+}], \\ \Psi_{\mathbf{k}}^2(\mathbf{r}) &= \frac{1}{\sqrt{C_2}} [\psi^{AC+} - i\psi^{BD+}], \end{aligned} \quad (19)$$

where C_1 and C_2 are normalization constants and the linear combinations $\psi^{AC+} = \psi^A + \psi^C$ and $\psi^{BD+} = \psi^B + \psi^D$ contain wave-functions with coefficients given in Table III. The wave-functions defined by Eq. (19) represent a complete system of eigenfunctions in the subspace characterized by $k = |\mathbf{k}|$ and the incident angle $\theta > \theta_c$. The symmetry between heavy-hole contributions with opposite helicity is reflected by the special relation between the corresponding coefficients, $c_2 = \pm i c_1$ and $c_6 = \pm i c_5$. The complete set of relations between the coefficients is given in Table IV.

	c_1^α	c_2^α	c_3^α	c_4^α	c_5^α	c_6^α
Ψ^1	c_1^1	ic_1^1	0	$(1+i)b_2^1$	$(c_1^1)^*$	$i(c_1^1)^*$
Ψ^2	c_1^2	$-ic_1^2$	$(1+i)b_1^2$	0	$(c_1^2)^*$	$-i(c_1^2)^*$

TABLE IV: Relations between the coefficients of the symmetric eigenstates in the presence of the localized modes, i.e. for an incident angle for the heavy-holes $\theta > \theta_c$. The wave functions for the eigenstates Ψ^1 and Ψ^2 given by Eq. (19) are expressed in the general form given by Eq. (18). The coefficients b_2^1 and b_1^2 are real. Notice that there are only two independent eigenstates for a given set of parameters (k, θ) , in contrast with the case $\theta < \theta_c$ when four independent eigenvectors were found.

We have identified complete sets of linearly independent eigenstates for arbitrary values of the incident momentum of the heavy-holes, i.e. for arbitrary parameters (k, θ) . These sets of eigenstates are given by the equations (14) and (19). In order to construct an orthonormal basis for the quantum problem defined by the Luttinger Hamiltonian in half-space, we have to solve two problems: a) the orthogonality of the eigenstates, and b) the proper counting of the modes. We address these issues in the remaining of this section.

A. Orthogonality of the symmetrized eigenstates

Let us start by clarifying a few aspects related to the definition of the scalar product that we use here. Consider two wave-functions $\Psi_{\mathbf{k}}^\alpha$ and $\Psi_{\mathbf{k}'}^{\alpha'}$ where $\mathbf{k} = (k_x, 0, k_z)$, with $k_x/k_z = -\tan(\theta)$, represents the momentum of the incident heavy-hole mode and $\alpha \in \{1+, 1-, 2+, 2-\}$, if $\theta < \theta_c$ or $\alpha \in \{1, 2\}$, if $\theta > \theta_c$. For reasons that will become clear below when we address the problem of counting the states, we consider a “discretized” momentum space so that two momenta are considered identical, $\mathbf{k} = \mathbf{k}'$, if they are both in a certain cell of volume δk^3 and different otherwise. We define the scalar product of the two states as

$$\langle \Psi_{\mathbf{k}}^\alpha | \Psi_{\mathbf{k}'}^{\alpha'} \rangle = \int_{\Omega} d^3r [\Psi_{\mathbf{k}}^\alpha(\mathbf{r})]^\dagger \Psi_{\mathbf{k}'}^{\alpha'}(\mathbf{r}), \quad (20)$$

where $\Omega = L^3$ is the volume of the system. We will always consider the thermodynamic limit $L \rightarrow \infty$, so that $L\delta k \gg 1$. Due to the particular form of the eigenfunctions (13) and (18), the integrations over x , y , and z can be performed separately. Due to our choice for the coordinate system, the wave-functions are independent of y and therefore the integration over this coordinate trivially generates a factor L . Further, all the x -dependence is contained in the factors $\exp(ik_x x)$ so that the x -integration generates a factor $L\delta_{k_x, k'_x}$. Consequently, Eq. (20) reduces to the one dimensional integral

$$\langle \Psi_{\mathbf{k}}^\alpha | \Psi_{\mathbf{k}'}^{\alpha'} \rangle = L^2 \delta_{k_x, k'_x} \int_0^L dz [\Psi_{\mathbf{k}}^\alpha(z)]^\dagger \Psi_{\mathbf{k}'}^{\alpha'}(z), \quad (21)$$

where $\Psi_{\mathbf{k}}^\alpha(z) = \Psi_{\mathbf{k}}^\alpha(\mathbf{r}) \exp(-ik_x x)$. We notice that, in order to insure convergence, all the z -dependent oscillatory terms in Eq. (21) are multiplied by a convergence factor $\exp(-\eta z)$ with $\eta L \gg 1$, and the limit $\eta \rightarrow 0$ is taken at the end of the calculation. Considering now the expressions (13) and (18) for the eigenfunctions, together with the properties of the coefficients summarized in Table II and Table IV, as well as the expressions for the spinors given in Appendix A, we obtain the generic expressions of the terms contributing to the scalar product (21). We will concentrate on the case $k_x = k'_x$, because for different x -components of the momentum the states are manifestly orthogonal. Also notice that, due to the exponential factors $\exp(-Qz)$, the localized modes from the eigenfunctions (18) will generate terms proportional to $1/(LQ)$, which vanish in the thermodynamic limit, and therefore will not contribute to the scalar products. Omitting these terms, the generic contribution to the integral over z in the scalar product has the form

$$L^2 [\Psi_{\mathbf{k}}^\alpha(z)]^\dagger \Psi_{\mathbf{k}'}^{\alpha'}(z) = \sum_{(k_1, k_2)} \frac{1}{L} \left[\Lambda_1^{\alpha, \alpha'}(k_1, k_2) \cos[(k_1 - k_2)z] + \Lambda_2^{\alpha, \alpha'}(k_1, k_2) \sin[(k_1 - k_2)z] \right], \quad (22)$$

with $(k_1, k_2) \in \{(k_z, \pm k'_z), (k_z, \pm q'_z), (q_z, \pm k'_z), (q_z, \pm q'_z)\}$, where k_z and k'_z are the z -components of the incident wave-vector for the heavy-hole modes, while q_z and q'_z are the z -components of the incident light-hole waves. The reflected waves have components with opposite signs. Due to the symmetry properties of the eigenstates, some of the coefficients $\Lambda_i^{\alpha, \alpha'}$ are identically zero. The non-vanishing coefficients are summarized in Table V. Integrating now Eq. (22) over z ,

	(1+)	(1-)	(2+)	(2-)	(1)	(2)
(1+)	Λ_1	Λ_2	Λ_1	Λ_2	Λ_1, Λ_2	Λ_1, Λ_2
(1-)	Λ_2	Λ_1	Λ_2	Λ_1	Λ_1, Λ_2	Λ_1, Λ_2
(2+)	Λ_1	Λ_2	Λ_1	Λ_2	Λ_1, Λ_2	Λ_1, Λ_2
(2-)	Λ_2	Λ_1	Λ_2	Λ_1	Λ_1, Λ_2	Λ_1, Λ_2
(1)	Λ_1, Λ_2	Λ_1, Λ_2	Λ_1, Λ_2	Λ_1, Λ_2	Λ_1, Λ_2	0
(2)	Λ_1, Λ_2	Λ_1, Λ_2	Λ_1, Λ_2	Λ_1, Λ_2	0	Λ_1, Λ_2

TABLE V: Non-vanishing $\Lambda_i^{\alpha, \alpha'}(k_1, k_2)$ coefficients that contribute to the scalar product of the eigenstates $\Psi_{\mathbf{k}}^\alpha(z)$ and $\Psi_{\mathbf{k}'}^{\alpha'}(z)$. The rows of the table are indexed by α and the columns by α' . For example, the scalar product of Ψ^{2+} and Ψ^{2-} will be an integral over z of a sum containing only Λ_2 -type terms. The simple z -dependence of the integrand, given by Eq. (22), and the properties of the coefficients $\Lambda_i^{\alpha, \alpha'}(k_1, k_2)$ enable us to prove the orthogonality of the eigenfunctions.

and taking the necessary limit for the convergence factor η , we obtain two types of contributions to the scalar product of two eigenstates $\Psi_{\mathbf{k}}^\alpha$ and $\Psi_{\mathbf{k}'}^{\alpha'}$: $\Lambda_1^{\alpha, \alpha'}(k_1, k_1)$ if $k_1 = k_2$ and $\frac{1}{L} \Lambda_2^{\alpha, \alpha'}(k_1, k_2)/(k_1 - k_2)$ if $k_1 \neq k_2$. For the contribution proportional to Λ_2 we distinguish two regimes. The first regime is characterized by a finite difference $k_1 - k_2$, so that $L|k_1 - k_2| \gg 1$, and occurs for example in combinations like $k_z + k'_z$ or $k_z + k'_z$. In this case there is no contribution to the scalar product in the thermodynamic limit. In the second regime, the difference between the two components of the wave-vector can be arbitrarily small, so that $k_1 \approx k_2$ and the ratio $\Lambda_2^{\alpha, \alpha'}(k_1, k_2)/(k_1 - k_2)$ seems to diverge. However, by evaluating explicitly the coefficients in this limit we obtain $\Lambda_2^{\alpha, \alpha'}(k_1, k_2) \propto k_1 - k_2$ and the corresponding contribution to the scalar product vanishes again in the thermodynamic limit. This behavior is valid for all cases, except when $(\alpha, \alpha') = (i\pm, j\mp)$ with $i \neq j$, for example in the case $k_z \approx k'_z$, $q_z \approx q'_z$ and $(\alpha, \alpha') = (1+, 2-)$. In these special cases when the Λ_2 terms do not vanish individually, a direct evaluation of the coefficients in the limit $k_z \rightarrow k'_z$ shows that

$$\frac{\Lambda_2^{\alpha, \alpha'}(q_z, q'_z)}{\Lambda_2^{\alpha, \alpha'}(k_z, k'_z)} = - \left| \frac{\partial q_z}{\partial k_z} \right| = - \frac{\xi |\cos(\theta)|}{\sqrt{\xi - \sin^2(\theta)}}. \quad (23)$$

Consequently, the total contribution to the scalar product, $\frac{1}{L}[\Lambda_2^{\alpha,\alpha'}(k_z, k'_z)/(k_z - k'_z) + \Lambda_2^{\alpha,\alpha'}(q_z, q'_z)/(q_z - q'_z)]$ vanishes again in the thermodynamic limit. The $\Lambda_1^{\alpha,\alpha'}(k_1, k_1)$ terms also vanish for $\alpha \neq \alpha'$. In fact, the only contributions to the scalar products that survive in the thermodynamic limit arise from $\Lambda_1^{\alpha,\alpha}(k_z, k_z)$ and $\Lambda_1^{\alpha,\alpha}(q_z, q_z)$ and we have

$$\begin{aligned}\Lambda_1^{\alpha,\alpha}(k_z, k_z) + \Lambda_1^{\alpha,\alpha}(q_z, q_z) &= \sum_{i=1}^8 |c_i^\alpha|^2 = 1 & \text{for } \theta < \theta_c, \\ \Lambda_1^{\alpha,\alpha}(k_z, k_z) &= |c_1^\alpha|^2 + |c_2^\alpha|^2 + |c_5^\alpha|^2 + |c_6^\alpha|^2 = 1 & \text{for } \theta > \theta_c,\end{aligned}\quad (24)$$

where the unity was obtained by a proper choice of the normalization constants for the coefficients c_i^α in the construction of the symmetrized states. We conclude that the symmetrized eigenstates constructed here represent an orthonormal system satisfying $\langle \Psi_{\mathbf{k}}^\alpha | \Psi_{\mathbf{k}'}^{\alpha'} \rangle = \delta_{\alpha\alpha'} \delta_{\mathbf{k}\mathbf{k}'}$.

B. Counting the eigenstates

The standard procedure for counting the states and transforming sums over the \mathbf{k} -vector into integrals for a quantum system in the thermodynamic limit consists in imposing periodic boundary conditions for a finite volume $\Omega = L^3$ system, and then taking the limit $L \rightarrow \infty$. The periodic boundary conditions generate a discrete set of wave-vectors $\mathbf{k} = (k_x, k_y, k_z) = 2\pi/L(n_1, n_2, n_3)$, where n_i are integers. The procedure works in the presence of spin-orbit coupling if no boundary is considered and the eigenstates are the heavy-hole and light-hole modes. However in our case, the eigenstates are certain combinations of heavy- and light-holes corresponding to the same energy. Explicitly, for $\theta < \theta_c$, heavy-hole modes with $\mathbf{k}_H = 2\pi/L(n_x, n_y, n_z)$ have to be paired up with light-holes characterized by the wave-vector $\mathbf{q}_L = 2\pi/L(n_x, n_y, m_z)$ with m_z satisfying

$$\xi \left(\frac{2\pi}{L} \right)^2 (n_x^2 + n_y^2 + n_z^2) = \left(\frac{2\pi}{L} \right)^2 (n_x^2 + n_y^2 + m_z^2). \quad (25)$$

For an arbitrary value of $\xi = m_L/m_H$ there is no integer solution of this equation. To overcome this difficulty we consider a partition of the reciprocal space with the property that all the heavy-hole modes characterized by helicity λ and wave-vectors situated in a cell δk^3 centered on \mathbf{k} are represented by a single heavy-hole mode (\mathbf{k}, λ) with the energy $\epsilon_k = k^2/2m_H$ and an effective ‘‘degeneracy’’ $\nu_0 = \delta k^3(L/2\pi)^3 \gg 1$. In the thermodynamic limit we can choose δk arbitrarily small, so that $1/\delta k$ is larger than any relevant length-scale in the problem. For incident angles $\theta < \theta_c$, the heavy-hole modes from a cell $(\mathbf{k}, \delta k^3)$ will pair with light-hole modes from a cell $(\mathbf{q}, \delta q^3)$, were all the points of the new cell were obtained by mapping the points of the original cell, $\mathbf{k} \rightarrow \mathbf{q}$, using Eq. (10). The ratio of the light-hole and heavy-hole degrees of freedom from the two cells is

$$R_{LH} = \frac{\delta q^3}{\delta k^3} = \left| \frac{\partial q_z}{\partial k_z} \right| = \frac{\xi |\cos(\theta)|}{\sqrt{\xi - \sin^2(\theta)}}. \quad (26)$$

For each heavy-hole mode with helicity $+3/2$ used in the construction of the eigenstates (14) we will use another heavy-hole with opposite helicity as well as $2R_{LH}$ light-hole modes and we will generate $2\mu_1$ states $\Psi_{\mathbf{k}}^{1\pm}$ and $2\mu_2$ states $\Psi_{\mathbf{k}}^{2\pm}$. The effective degeneracies μ_i are determined by the condition that, far from the boundary, the number of heavy- and light-hole modes is the same as in an infinite system. Consequently we have

$$\begin{aligned}\mu_1 W_{HH}^{1\pm} + \mu_2 W_{HH}^{2\pm} &= 1, \\ \mu_1 W_{LH}^{1\pm} + \mu_2 W_{LH}^{2\pm} &= R_{LH},\end{aligned}\quad (27)$$

where W_{LH} and W_{HH} are the light-hole and heavy-hole weights, respectively. We obtain for the effective degeneracies of the eigenstates $\Psi_{\mathbf{k}}^{i\sigma}$ given by (14) the expressions

$$\mu_1 = \frac{1 - W_{HH}^{2\sigma}(1 + R_{LH})}{W_{HH}^{1\sigma} - W_{HH}^{2\sigma}}, \quad \mu_2 = 1 + R_{LH} - \mu_1. \quad (28)$$

Notice that these expressions are meaningful only if the effective degeneracies satisfy the condition $0 \leq \mu_i \leq (1 + R_{LH})$. Consequently, the weights of the heavy-hole modes contained in eigenstates defined by equations (14) cannot be arbitrary. If, for example, $W_{HH}^{1\sigma} > W_{HH}^{2\sigma}$ they have to satisfy the inequalities

$$W_{HH}^{1\sigma} > \frac{1}{1 + R_{LH}}, \quad W_{HH}^{2\sigma} < \frac{1}{1 + R_{LH}}. \quad (29)$$

These inequalities are the reason behind our choice for the parameter 'a' in the construction of the eigenstates (14). By maximizing the weight of the heavy-holes in the type-1 eigenstates and minimizing it in the type-2 eigenstates we insure that the inequalities (29) are always satisfied. The analysis of the case $\theta > \theta_c$ is straightforward, because far from the boundary only the heavy-hole modes survive. Consequently, there is a direct correspondence between the number of degrees of freedom associated with the heavy-holes and the number of symmetrized eigenstates (19).

In this section we have constructed an orthonormal basis for the Luttinger Hamiltonian in half space. For our particular choice of coordinates, the basis consists in the symmetrized eigenfunctions $\Psi_{\mathbf{k}}^{i\sigma}$ given by equations (14) with $i = 1, 2$, $\sigma = \pm$, and $\mathbf{k} = (k_x, 0, k_z)$ for incident angles $\theta = -\arccos(k_z/k) < \theta_c$, together with the eigenstates $\Psi_{\mathbf{k}}^i$ given by Eq. (19) with $i = 1, 2$ and incident angles $\theta = -\arccos(k_z/k) > \theta_c$. The eigenstates from the first set have an effective degeneracy $\nu_0\mu_i$ with μ_i given by (28), while the eigenstates from the second set have an effective degeneracy ν_0 in our discretization construction for the momentum space. Notice that the overall factor ν_0 is irrelevant in the calculation of the physical quantities. We conclude this section by giving the rules for transforming sums over the k-vector into integrals. Let us assume that $f(\mathbf{k}, \alpha)$ is a function that depends on the diagonal matrix elements $\langle \Psi_{\mathbf{k}}^\alpha | A | \Psi_{\mathbf{k}}^\alpha \rangle$ of a certain operator A and that we are interested in calculating its sum over all the eigenstates of the basis. We have

$$\sum_{\mathbf{k}} \sum_{i,\sigma}^{(\theta < \theta_c)} (\nu_0\mu_i) f(\mathbf{k}, i, \sigma) + \sum_{\mathbf{k}} \sum_i^{(\theta > \theta_c)} (\nu_0) f(\mathbf{k}, i) = \frac{\Omega}{(2\pi)^3} \sum_{i,\sigma} \int_{(\theta < \theta_c)} d^3k \mu_i f(\mathbf{k}, i, \sigma) + \frac{\Omega}{(2\pi)^3} \sum_i \int_{(\theta > \theta_c)} d^3k f(\mathbf{k}, i), \quad (30)$$

where we have taken into account that the volume of a cell in the discretized momentum space is $\delta k^3 = \nu_0(2\pi/L)^3$ and we have considered the thermodynamic limit $L \rightarrow \infty$. For example if $f(\mathbf{k}, \alpha)$ represents the occupation number at zero temperature of the mode with the quantum numbers (\mathbf{k}, α) , by applying Eq. (30) we can easily obtain the relation between the Fermi k-vector and the density of particles, $n = k_F^3(1 + \xi^{\frac{3}{2}})/(6\pi^2)$. Notice that each component $\Psi_{\mathbf{k}}^\alpha$ of the basis, although contains a superposition of heavy- and light-holes, is labeled by the k-vector of the incident heavy-hole mode and has an energy $\epsilon_k = k^2/(2m_H)$ independent of α . Consequently, the Fermi wave-vector k_F is independent of α and is determined by the density of particles and the spin-orbit coupling.

III. OSCILLATING SPIN DENSITY AND SPIN ACCUMULATION

In this section we investigate the properties of the spin density and explore the possibility of spin accumulation in a system with a sharp boundary described by the Luttinger model (here and below we actually study the accumulation of the total orbital momentum, but we call it "spin accumulation" for brevity). We can derive the spin density from the one-particle propagators. Using the orthonormal basis constructed in the previous section, we can define the Green's functions for the Luttinger model in half space. The retarded Green's function is

$$G_{ab}^{(R)}(\omega; \mathbf{r}, \mathbf{r}') = \sum_{\mathbf{k}, \alpha} \nu_{k\alpha} \frac{[\Psi_{\mathbf{k}}^\alpha(\mathbf{r}')]^*_b [\Psi_{\mathbf{k}}^\alpha(\mathbf{r})]_a}{\omega - \mu - \epsilon_k + i0^+}, \quad (31)$$

where μ is the chemical potential and $\Psi_{\mathbf{k}}^\alpha(\mathbf{r})$ is a vector from the basis defined by the equations (14) and (18) corresponding to the eigenvalue $\epsilon_k = k^2/2m_H$, with m_H being the heavy-hole mass. The eigenvectors are labeled by the wave-vector \mathbf{k} of the incident heavy-hole mode and the index α which takes four values, $\alpha \in \{1+, 1-, 2+, 2-\}$, if all the modes propagate in the z-direction ($\theta < \theta_c$), and two values, $\alpha \in \{1, 2\}$, if the eigenstate contains localized modes ($\theta > \theta_c$). In addition, because the states $\Psi_{\mathbf{k}}^\alpha(\mathbf{r})$ are four-component spinors, we have the indices a and b to label their components. Finally, to correctly account for the light- and heavy-hole modes used in the construction of the basis, we have the effective degeneracy factor $\nu_{k\alpha} = \nu_0\mu_\alpha$, where μ_α is given by Eq. (28) when the eigenvector contains only propagating modes, i.e. for $\theta < \theta_c$, and $\mu_\alpha = 1$ otherwise, while $\nu_0 = \delta k^3/(2\pi/L)^3$ is determined by our momentum discretization procedure (as we have noted above this factor drops out of all final results). The density of the total momentum \mathbf{S} can be expressed in terms of Green's function as $\langle \mathbf{S} \rangle(\mathbf{r}) = -i \int d\omega \text{Tr}[\hat{\mathbf{S}} \hat{G}(\omega; \mathbf{r}, \mathbf{r})]$, where the matrices $\mathbf{S}_{ab} = ([S_x]_{ab}, [S_y]_{ab}, [S_z]_{ab})$ are given in Appendix A. In terms of the eigenstates for the Luttinger model in half-space we have explicitly

$$\langle S_l \rangle(\mathbf{r}) = \sum_{\mathbf{k}} \sum_{\alpha} \nu_{k\alpha} \left([\Psi_{\mathbf{k}}^\alpha(\mathbf{r})]^\dagger \hat{S}_l \Psi_{\mathbf{k}}^\alpha(\mathbf{r}) \right) n_\alpha(\mathbf{k}), \quad (32)$$

where \hat{S}_l is the matrix for the $l \in \{x, y, z\}$ component of the total momentum, $n_\alpha(\mathbf{k}) \in \{0, 1\}$ is the zero temperature occupation number of the $\Psi_{\mathbf{k}}^\alpha$ state with effective degeneracy $\nu_{k\alpha}$, and the summations, which include all the eigenstates

in the basis, can be converted into integrals using Eq. (30). The analysis can be greatly simplified if we take into account the symmetry properties of the eigenstates. These symmetries translate directly into relations between single state contributions to the matrix element of the spin density,

$$\mathcal{S}_i^\alpha(\mathbf{k}, \mathbf{r}) = [\Psi_{\mathbf{k}}^\alpha(\mathbf{r})]^\dagger \hat{S}_i \Psi_{\mathbf{k}}^\alpha(\mathbf{r}). \quad (33)$$

Explicitly we have

$$\begin{cases} \mathcal{S}_x^{i\sigma}(\mathbf{k}, \mathbf{r}) = -\mathcal{S}_x^{i(-\sigma)}(\mathbf{k}, \mathbf{r}) & \text{for } \theta < \theta_c, \\ \mathcal{S}_x^i(\mathbf{k}, \mathbf{r}) = 0 & \text{for } \theta > \theta_c, \\ \mathcal{S}_z^{i\sigma}(\mathbf{k}, \mathbf{r}) = 0 & \text{for } \theta < \theta_c, \\ \mathcal{S}_z^i(\mathbf{k}, \mathbf{r}) = 0 & \text{for } \theta > \theta_c, \end{cases} \quad (34)$$

where $i = 1, 2$ and $\sigma = \pm$ represent the labels of the corresponding eigenstates. We conclude that the contribution to the x and z-components of the spin density from any wave-vector \mathbf{k} is identically zero. On the other hand, for the y-component we obtain

$$\begin{cases} \mathcal{S}_y^{i\sigma}(\mathbf{k}, \mathbf{r}) = \mathcal{S}_y^{i(-\sigma)}(\mathbf{k}, \mathbf{r}) & \text{for } \theta < \theta_c, \\ \mathcal{S}_y^1(\mathbf{k}, \mathbf{r}) = \mathcal{S}_y^2(\mathbf{k}, \mathbf{r}) & \text{for } \theta > \theta_c, \end{cases} \quad (35)$$

and consequently we get in general a non-zero total contribution for a given \mathbf{k} . In other words, in a system described by the Luttinger Hamiltonian and having a sharp planar boundary, the contribution to the spin density vector from states characterized by a wave-vector \mathbf{k} is oriented along a direction parallel to the boundary and perpendicular to the wave-vector, $\vec{\mathcal{S}}(\mathbf{k}, \mathbf{r}) \propto \mathbf{n}_b \times \mathbf{k}$, where \mathbf{n}_b is a unit vector normal to the boundary. We remind here that the eigenfunctions $\Psi_{\mathbf{k}}^\alpha$ are written in the ‘‘local’’ coordinate system determined by the convention $\mathbf{k} = (k_x > 0, 0, k_z)$, and therefore, whenever we have to use a system of coordinates independent of \mathbf{k} , special attention should be given to the transformation rules. In particular, for the spin density vector we have

$$\vec{\mathcal{S}}((k_x, k_y, k_z), \mathbf{r}) = -\vec{\mathcal{S}}((-k_x, -k_y, k_z), \mathbf{r}), \quad (36)$$

i.e. the contributions to the matrix element (33) from wave-vectors with opposite components parallel to the surface have the same length and opposite orientations. Consequently, in the ground-state the spin-density vanishes. However, it is possible to generate a non-vanishing spin-density if the number of particles moving in one direction is different from the number of particles moving in the opposite direction, i.e. in the presence of a charge current parallel to the boundary.

Let us assume now that the system is characterized by a preferential direction of motion for the carriers imposed by an external current flowing in the x-direction and having the average current density $\langle j_x \rangle$. We reiterate that if the system is perfectly clean and an external electric field is present, then the particles will just accelerate indefinitely and the spin density will be time-dependent. This scenario is not considered here. Below we study the situations when the equilibrium current appears either due to a voltage drop which occurs entirely in the contacts, or because some disorder is present. In the latter case, we study only the lengthscales much smaller than the mean-free path (the physics at larger length-scales in disordered systems will be discussed in Sec. IV). We can associate the current with a drift velocity $\mathbf{v}_0 = (\Delta k/m_H, 0, 0)$ with $\Delta k \ll k_F$, and assume that the distribution function for the system changes from $n^0(\mathbf{k}) = \Theta(\epsilon_F - \epsilon_{\mathbf{k}})$ to $n(\mathbf{k}) = \Theta(\epsilon_F - \epsilon_{\mathbf{k} + \Delta \mathbf{k}})$, where $\Theta(x)$ is the step function, $\epsilon_{\mathbf{k}} = k^2/2m_H$ are the energies of the eigenstates, and ϵ_F is the Fermi energy corresponding to the Fermi wave-vector k_F related to the density of particles, $n = k_F^3(1 + \xi^{\frac{3}{2}})/(6\pi^2)$. Using the relation (30) of transforming the sums over \mathbf{k} into integrals, we have

$$\langle j_x \rangle = \frac{1}{4\pi^3} \frac{e\hbar}{m_H} \left\{ \int_{\theta < \theta_c} d^3k [1 + R_{LH}(\mathbf{k})] k_x n(\mathbf{k}) + \int_{\theta > \theta_c} d^3k k_x n(\mathbf{k}) \right\} = \frac{e\hbar}{m_H} \frac{1 + \xi^{\frac{5}{2}}}{1 + \xi^{\frac{3}{2}}} n \Delta k, \quad (37)$$

where n is the average particle density of the system and we have taken into account that the drift velocity is much smaller than the Fermi velocity. In the presence of the external current, the y-component of the spin density becomes non-zero and, using the definition (32) together with Eq. (30), we have

$$\begin{aligned} \langle S_y \rangle(\mathbf{r}) &= \frac{1}{(2\pi)^3} \left\{ \sum_{\sigma} \int_{\theta < \theta_c} d^3k [\mu_1(\theta) \mathcal{S}_y^{1\sigma}(\theta, \mathbf{r}) + \mu_2(\theta) \mathcal{S}_y^{2\sigma}(\theta, \mathbf{r})] \cos(\phi) n(\mathbf{k}) \right. \\ &\quad \left. + \int_{\theta > \theta_c} d^3k [\mathcal{S}_y^1(\theta, \mathbf{r}) + \mathcal{S}_y^2(\theta, \mathbf{r})] \cos(\phi) n_{\mathbf{k}} \right\} = \frac{k_F^2 \Delta k}{8\pi^2} \left\{ \int_0^{\theta_c} d\theta \mathcal{S}_{<}(\theta, z) + \int_{\theta_c}^{\pi/2} d\theta \mathcal{S}_{>}(\theta, z) \right\}, \end{aligned} \quad (38)$$

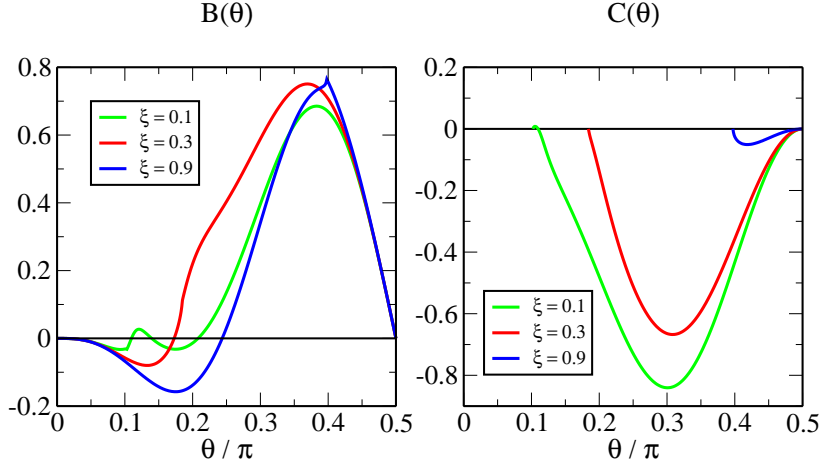


FIG. 5: (Color online) Angle dependence of the coefficients for the spin density defined by equations (42) and (43). The critical angles corresponding to the values of the mass ratio $\xi = 0.1, 0.3, 0.9$ are $\theta_c = 0.1024\pi, 0.1845\pi$ and 0.3975π , respectively.

where μ_i is the effective degeneracy of the eigenstate, $n(\mathbf{k}) = \Theta(\epsilon_F - \epsilon_{\mathbf{k}+\Delta\mathbf{k}})$, ϕ is the angle between the x-axis and the projection of the wave-vector on the x-y plane, and the factor $\cos(\phi)$ is due to the fact that $\mathcal{S}_y^\alpha(\theta, \mathbf{r})$ is calculated in the local coordinate system. Finally, the functions integrated over the angle θ in the last member of Eq. (38) are

$$\mathcal{S}_<(\theta, z) = 2 [\mu_1(\theta)\mathcal{S}_y^{1+}(\theta, z) + \mu_2(\theta)\mathcal{S}_y^{2+}(\theta, z)] \sin^2(\theta) \quad \text{and} \quad \mathcal{S}_>(\theta, z) = [\mathcal{S}_y^1(\theta, z) + \mathcal{S}_y^2(\theta, z)] \sin^2(\theta). \quad (39)$$

As expected, the spin density is proportional to Δk , i.e. to the average density of the external current. So far, we have reduced the expression for the spin density $\langle S_y \rangle(\mathbf{r})$ to a sum of one dimensional integrals over the incident angle θ . Furthermore, we can write explicitly the z-dependence of $\mathcal{S}(\theta, z)$ using the expressions for the wave-functions and spinors as well as the symmetry properties of the coefficients. We obtain

$$\begin{aligned} \mathcal{S}_<(\theta, z) &= B(\theta) \left\{ \sin[2\tilde{k}_z z] + \sin[2\tilde{q}_z z] - 2 \sin[(\tilde{k}_z + \tilde{q}_z)z] \right\}, \\ \mathcal{S}_>(\theta, z) &= B(\theta) \left\{ \sin[2\tilde{k}_z z] - 2 \sin[\tilde{k}_z z] e^{-\tilde{Q}z} \right\} + C(\theta) \left\{ \cos[2\tilde{k}_z z] + e^{-2\tilde{Q}z} - 2 \cos[\tilde{k}_z z] e^{-\tilde{Q}z} \right\}, \end{aligned} \quad (40)$$

where the wave-vectors are proportional to k_F and depend on the incident angle θ . Explicitly we have

$$\begin{aligned} \tilde{k}_z &= k_F \cos(\theta), \\ \tilde{q}_z &= k_F \sqrt{\xi - \sin^2(\theta)}, & \theta < \theta_c, \\ \tilde{Q} &= k_F \sqrt{\sin^2(\theta) - \xi}, & \theta > \theta_c. \end{aligned} \quad (41)$$

The complete information about the spin density is contained in the coefficients $B(\theta)$ and $C(\theta)$. These quantities can be expressed in terms of the coefficients c_i^α of the symmetric eigenfunctions (14) and (18). Explicitly, we have for $\theta < \theta_c$:

$$B(\theta) = -6 \left\{ \mu_1 [(c_1^1)^2 - (c_2^1)^2] + \mu_2 [(c_1^2)^2 - (c_2^2)^2] \right\} \cos(\theta) \sin^4(\theta) - 12 [\mu_1 c_1^1 c_2^1 + \mu_2 c_2^1 c_2^2] \cos^2(\theta) \sin^3(\theta), \quad (42)$$

where μ_i are the effective degeneracies given by equation (28) and the notations for the coefficients c_i^α are taken from Table II. Similarly, for $\theta > \theta_c$ we have

$$\begin{aligned} B(\theta) &= -6 \text{Re} [(c_1^1)^2 + (c_1^2)^2] \cos(\theta) \sin^4(\theta) + 6 \text{Re} [i(c_1^1)^2 - i(c_1^2)^2] \cos^2(\theta) \sin^3(\theta) \\ C(\theta) &= 6 \text{Im} [(c_1^1)^2 + (c_1^2)^2] \cos(\theta) \sin^4(\theta) - 6 \text{Im} [i(c_1^1)^2 - i(c_1^2)^2] \cos^2(\theta) \sin^3(\theta), \end{aligned} \quad (43)$$

where the notations for the coefficients c_i^α are taken from Table IV. The explicit dependence of the coefficients B and C on θ is shown in Fig. 5 for several values of the mass ratio ξ . Notice that the coefficient $C(\theta)$ vanishes at the critical angle $\theta = \theta_c$ and at $\pi/2$, while $B(\theta)$ vanishes at $\theta = 0, \pi/2$ and has a singularity at the critical angle characterized by a discontinuity of the first derivative. Knowing these coefficients, we can perform the integral over the angle θ in

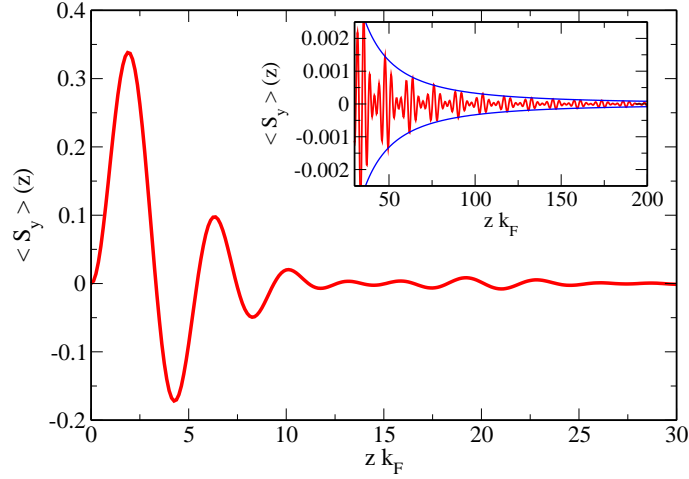


FIG. 6: (Color online) Position dependence of the current-induced spin density $\langle S_y \rangle$ expressed in units of $k_F^2 \Delta k / 8\pi^2$ for a mass ratio $\xi = 0.3$ relevant for a GaAs system. The inset shows the large- z behavior characterized by a decay of the oscillations proportional to $1/z^2$ (blue lines).

Eq. (38) and obtain the spin density. The result for $\xi = 0.3$ is shown in Fig. 6 revealing several interesting features. It confirms that the current-induced spin density is indeed non-zero. In fact the spin density oscillates about zero with an amplitude that vanishes as we move away from the boundary. The oscillations are characterized by several wave-lengths, as shown by the beat phenomenon in the inset of Fig. 6. On the other hand, the amplitude of the oscillations decreases as $1/z^2$ at large distances. All these features are contained in the properties of the coefficients $B(\theta)$ and $C(\theta)$, in particular in their behavior in the vicinity of the singular points $\theta = 0, \theta_c$ and $\pi/2$. Below, we will analyze in detail the connection between these singular points and the oscillating properties of the spin density.

A. The asymptotic behavior of the spin density

The amplitude and the period of the spin density oscillations far from the boundary are completely determined by the singular points of the coefficients $B(\theta)$ and $C(\theta)$. To prove this, let us consider as an example one of the terms from Eq. (40) and re-write the corresponding contribution to the spin density as a Fourier transform,

$$\int_0^{\theta_c} d\theta B(\theta) \sin(2\tilde{k}_z z) = \int_{-\infty}^{\infty} dp b(p) \sin(pz), \quad (44)$$

where

$$b(p) = \begin{cases} \frac{B(\arccos(\frac{p}{2k_F}))}{\sqrt{4-p^2}} & \text{if } 0 \leq p \leq 2\sqrt{1-\xi}, \\ 0 & \text{otherwise.} \end{cases} \quad (45)$$

If the Fourier coefficient $b(p)$ has a singularity at $p_0 \neq 0$ characterized by a discontinuity $\Delta b^{(n)}(p_0)$ in the derivative of order n , the large- z behavior of the integral (44) is $\Delta b^{(n)}(p_0) \cos(p_0 z + n\pi/2) / z^{n+1}$, i.e. it oscillates with a period $\lambda = 2\pi/p_0$ and an amplitude which is proportional to the discontinuity in the derivative and decays as $1/z^{n+1}$. Similar relations can be established for cases when the discontinuity is not finite. For example, when the singularity is proportional to $\sqrt{p-p_0}$, the asymptotic behavior becomes $\cos(p_0 z + \pi/4) / z^{3/2}$. Returning now to the analysis of the contributions to the spin density coming from Eq. (40), we notice that the possible singularities are given by the angles $\theta \in \{\pi/2, \theta_c, 0\}$. As $\tilde{k}_z(\theta = \pi/2) = 0$, there is no large- z contribution to the spin density coming from the states with the incident angle $\theta = \pi/2$. In other words, the modes propagating parallel to the boundary do not contribute to the spin density at positions far from the surface of the system. On the other hand, the critical angle θ_c requires a detailed evaluation. We should remind that, as shown in the inset of Fig. 6, the spin density oscillation decay as $1/z^2$. From Eq. (40) we observe that there are eight different terms that contribute to the spin density, three coming from $\mathcal{S}_<$ and five coming from $\mathcal{S}_>$. However, one can show that the contributions coming from the last

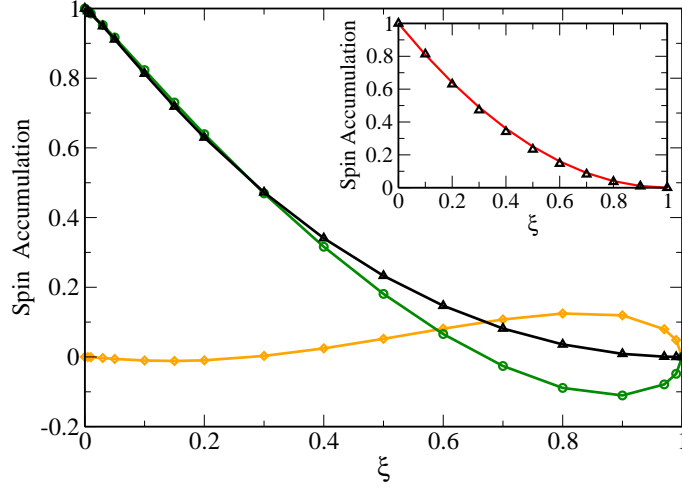


FIG. 7: (Color online) Total spin accumulation in units of $k_F \Delta k / 8\pi^2$ as a function of the mass ratio ξ (black line with triangles). The contributions from angles $\theta < \theta_c$ (orange line with diamonds) and $\theta > \theta_c$ (green line with circles) are shown separately. The inset represents a fit of the total spin accumulation (triangles) with the function $(1 - \xi)^2$ (continuous red line).

two terms proportional to $C(\theta)$ decay faster than $1/z^2$ and, consequently, can be neglected. The remaining six terms will give contributions that decay as $1/z^2$ or slower. For example, the first term $B(\theta) \sin(\tilde{k}_z z)$ with $\theta < \theta_c$ generates a contribution proportional to $B(\theta_c) \cos(2\sqrt{1-\xi}z)/z$ due to the fact that $B(\theta_c) \neq 0$. However, this contribution is exactly canceled by the corresponding contribution coming from the fourth term, $B(\theta) \sin(\tilde{k}_z z)$ with $\theta > \theta_c$. Similarly, the $\sqrt{\theta_c - \theta}$ term from $B(\theta)$ generates the contribution $\cos(2\sqrt{1-\xi}z + \pi/4)/z^{3/2}$, which is exactly canceled by the contribution generated by $C(\theta)$. In fact, one can show that there is no net contribution to the asymptotic spin density of order up to $\mathcal{O}(1/z^2)$ coming from the critical angle. This exact cancellation is embedded in the properties of the coefficients $B(\theta)$ and $C(\theta)$ in the vicinity of θ_c . Explicitly, for $\theta \approx \theta_c$ we have

$$\begin{aligned}
 B(\theta) &= \beta_0 + \beta_{1/2} \sqrt{\theta_c - \theta} + \beta_1 (\theta_c - \theta) + \mathcal{O}((\theta_c - \theta)^{3/2}), & \theta < \theta_c \\
 B(\theta) &= \beta_0 - \beta_1 (\theta - \theta_c) + \mathcal{O}((\theta - \theta_c)^2), & \theta > \theta_c \\
 C(\theta) &= \beta_{1/2} \sqrt{\theta - \theta_c} + \mathcal{O}((\theta - \theta_c)^{3/2}), & \theta > \theta_c.
 \end{aligned} \tag{46}$$

We conclude that the asymptotic behavior of the spin density is determined entirely by the modes propagating along the direction perpendicular to the boundary. The characteristic wave-vectors corresponding to the first three terms in Eq. (40) are $2k_z(0) = 2k_F$, $2\tilde{q}_z(0) = 2k_F \sqrt{\xi}$ and $\tilde{k}_z(0) + \tilde{q}_z(0) = k_F(1 + \sqrt{\xi})$. On the other hand, the amplitude is determined by the small angle behavior of the coefficient B , namely

$$B(\theta) = -3\theta^3 + \mathcal{O}(\theta^5), \quad \text{for } \theta \rightarrow 0. \tag{47}$$

Writing each term as a Fourier transform and using the properties discussed above in connection with equations (44-45) we obtain the following expression for the spin density far from the boundary

$$\langle S_y \rangle(z) = \frac{\Delta k}{8\pi^2} \frac{3}{2z^2} \left\{ \sin(2k_F z) + \xi \sin(2k_F \sqrt{\xi} z) - \frac{8\sqrt{\xi}}{(1 + \sqrt{\xi})^2} \sin[k_F(1 + \sqrt{\xi})z] \right\}, \quad zk_F \gg 1, \tag{48}$$

where the Fermi wave-vector is determined by the density and the spin-orbit coupling, $k_F = [6\pi^2 n / (1 + \xi^{3/2})]^{1/3}$. We note that the result (48) is asymptotically exact.

B. The spin accumulation

An important question is whether there is a net spin accumulation in the system. To answer this question, we first define the spin accumulation as an integral of the spin density with respect to the distance from the boundary

$$\bar{S}_y(z) = \int_0^z \langle S_y \rangle(\zeta) d\zeta. \tag{49}$$

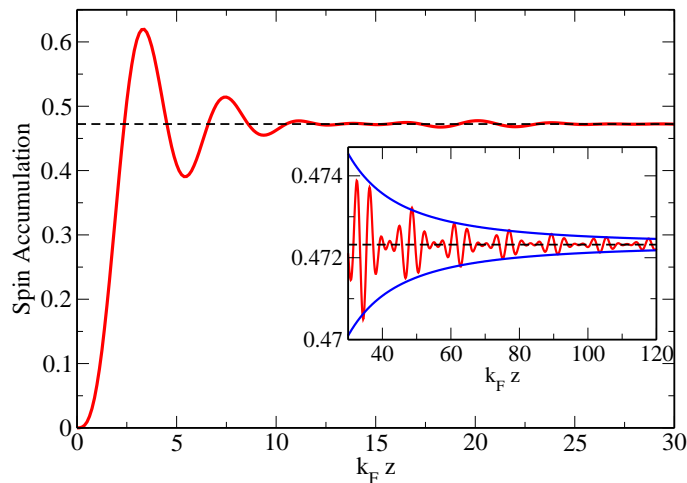


FIG. 8: (Color online) Current-induced spin accumulation in units of $k_F \Delta k / 8\pi^2$ as a function of the distance from the boundary. The curve was determined for $\xi = 0.3$ by integrating the data from Fig. 6 with respect to z from zero to a certain distance from the boundary. Notice that the spins are localized within a few Fermi lengths $\lambda_F = 2\pi/k_F$ off the boundary. The dashed line represents the total spin accumulation \bar{S}_y using the same units. The inset shows the $1/z^2$ decay of the fluctuations about \bar{S}_y at distances far from the boundary.

Here $\bar{S}_y(z)$ is the spin accumulation at a distance z from the boundary, more precisely the spin density per unit area. The total spin accumulation is $\bar{S}_y = \bar{S}_y(\infty)$. To determine the total spin accumulation it is convenient to perform first the integration over the coordinate z for each of the terms contributing to $\mathcal{S}(\theta, z)$. We obtain for the total spin accumulation the expression

$$\bar{S}_y = \int_0^{\theta_c} d\theta B(\theta) \left[\frac{1}{2\tilde{k}_z} + \frac{1}{2\tilde{q}_z} - \frac{2}{\tilde{k}_z + \tilde{q}_z} \right] + \int_{\theta_c}^{\pi/2} d\theta \left\{ B(\theta) \left[\frac{1}{2\tilde{k}_z} + \frac{\tilde{k}_z}{\tilde{k}_z^2 + \tilde{Q}^2} \right] + C(\theta) \left[\frac{1}{2\tilde{Q}} - \frac{2\tilde{Q}}{\tilde{k}_z^2 + \tilde{Q}^2} \right] \right\}, \quad (50)$$

where the dependence on θ of the wave-vectors \tilde{k}_z , \tilde{q}_z and \tilde{Q} is given by Eq. (41). Finally, the integration over the angle is performed numerically. The result for the spin accumulation as a function of the mass ratio $\xi = m_L/m_H$ is shown in Fig. 7. The spin accumulation decreases monotonically with ξ and vanishes in the absence of spin-orbit coupling ($\xi = 1$). We have also calculated separately the contributions from the angles smaller than the critical angle θ_c (orange line in Fig. 7) and the angles larger than θ_c (green line). For strong to intermediate values of the spin-orbit interaction practically the entire contribution to the spin accumulation comes from states with $\theta > \theta_c$, i.e. the states containing localized modes. In contrast, in the weak-coupling regime ($\xi \sim 1$), the two contributions are comparable and have opposite signs. Finally, we notice that the ξ -dependence of the total spin accumulation can be perfectly fitted as (see the inset in Fig. 7)

$$\bar{S}_y \approx \frac{k_F \Delta k}{8\pi^2} (1 - \xi)^2. \quad (51)$$

The spin accumulation as a function of distance has also been calculated numerically and the result is shown in Fig. 8. We see that the spin accumulation is localized in the vicinity of the boundary. The shortest distance from the boundary at which the spin accumulation becomes equal to the total spin accumulation \bar{S}_y is of the order of $2/k_F$, while at larger distances it oscillates about \bar{S}_y with an amplitude that decreases as we move away from the boundary. As shown in the inset of Fig. 8, at large distances the oscillations of the spin accumulation decay as $1/z^2$.

IV. THE EFFECTS OF DISORDER

A. The Friedel oscillations in a disordered system

In this section we qualitatively discuss the effects of disorder on the current-induced Friedel oscillations of the spin density. To understand these effects it is useful to recall the corresponding physics in the usual disordered Fermi

systems: Consider a perturbation (such as a boundary or an impurity) introduced in a Fermi gas. This perturbation leads to the Friedel oscillations in the electron density, which in a clean case behaves as $n(r) = Ar^{-p(d)} \cos(2p_F r)$, where r is the distance from the perturbation, A is a constant amplitude, and the power $p(d) = (d+1)/2$, if the perturbation is a boundary and $p(d) = d$, if the perturbation is point-like (i.e., a magnetic impurity). What happens with the Friedel oscillations if we introduce disorder? A natural quantity to calculate is the perturbation-induced density averaged over disorder realizations. As was shown by de Gennes,²³ it decays exponentially as $\langle n(\mathbf{r}) \rangle \propto e^{-r/l}$, where l is the mean free path. However, Zyuzin and Spivak²⁴ later argued that this result is misleading. Indeed, if we measure the density at different points but at the same distance away from the perturbation, we will get different results (in magnitude and sign), which will strongly depend on the local disorder realization (see also, Refs. [25, 26]). Therefore a more meaningful quantity is the full probability distribution function of density at a distance r from the perturbation $P[n, r]$. One should note that this probability distribution function is not known explicitly even in the simplest cases and only its lowest moments are available. The important result of Zyuzin and Spivak²⁴ (obtained in the context of RKKY oscillations between magnetic impurities in disordered metals) concerns the second moment, which was shown to decay as a power law, $\langle n(\mathbf{r})n(\mathbf{r}) \rangle \propto r^{-p(d)}$ just like in the clean case. The qualitative explanation of this result is that disorder effectively introduces random phase shifts $\delta(l)$ in the argument of the cosine in the Friedel oscillations $\propto \cos[2p_F r + \delta(l)]$. Averaging over disorder realizations leads effectively to the vanishing density due to the oscillations in the cosine. However, averaging of the cosine squared yields a finite result and restores the power law behavior of the *typical* Friedel oscillation.

To connect the above-mentioned arguments with our case, we mention that the higher moments of the probability distribution function of the Friedel oscillations in the density are described diagrammatically by bubble diagrams with all possible disorder averagings between them. A careful treatment of these diagrams reveals that the power-law (non-exponential) decay of the usual Friedel oscillations is due to the gapless nature of the diffusons of which these diagrams are built. Now let us return to the Friedel oscillations in the spin density and spin accumulation, which were discussed above in the clean case. A straightforward calculation shows that the spin density averaged over disorder decays exponentially as

$$\overline{\mathbf{S}(\mathbf{r})} \propto \int d\varepsilon \text{Tr} \left[\hat{\mathbf{S}} \hat{\mathbf{G}}(\varepsilon; \mathbf{r}, \mathbf{r}) \right] \propto e^{-r/l}, \quad (52)$$

where l is the mean free path, $\hat{\mathbf{G}}(\varepsilon; \mathbf{r}, \mathbf{r})$ is the Green's function which takes into account the boundary, and overline implies disorder averaging. Higher moments of the spin density are described by expressions, which involve different components of the diffuson. In particular, the second moment (correlator of spin densities) reads

$$\overline{S_\alpha(\mathbf{r})S_\alpha(\mathbf{r})} \propto \int d\varepsilon_1 \int d\varepsilon_2 \text{Tr} \left[\hat{S}_\alpha \hat{\mathbf{G}}(\varepsilon_1; \mathbf{r}, \mathbf{r}) \right] \text{Tr} \left[\hat{S}_\alpha \hat{\mathbf{G}}(\varepsilon_2; \mathbf{r}, \mathbf{r}) \right] \propto \frac{1}{r^4}, \quad (53)$$

We emphasize that due to the two traces present in Eq. (53), the correlation function includes contributions from different components of the diffuson matrix. Most importantly it contains a singlet component, which remains gapless even in a spin-orbit coupled system (see below subsection IV B). Therefore, the *typical* spin density measured at a distance $r \gg l$ from the boundary is expected to decay as a power law even if disorder is present. This spin density is however random in sign and can be estimated as $S_y(\mathbf{r}) \propto z^{-2} \sin[\phi_r(\mathbf{r})]$, where z is the distance from the boundary and ϕ_r is a random phase. Due to this randomness, the spin accumulation (i.e. the spin density averaged over the length-scales much larger than the Fermi-wavelength) is expected to decay exponentially as $\propto e^{-z/L_s}$, where L_s is the spin relaxation or spin diffusion length.^{10,27,28} We note that in the framework of the Luttinger model, the spin-orbit coupling is always strong and therefore the spin relaxation length is expected to be very short and of the order of the mean free path. We study the related spin relaxation time in the following subsection.

B. Spin relaxation time in the Luttinger model

For the sake of completeness, we calculate explicitly the spin relaxation time and find that it is very short (of order τ). Therefore, the spin relaxation length is short too and the hydrodynamic diffusion approximation is not applicable for spin transport in the Luttinger model. However, we believe that it is likely that the result for the spin relaxation time itself is quantitatively correct and describes time relaxation of a uniform spin distribution.

To find the spin relaxation time, we construct the diffuson, which can be obtained from a convolution of disorder-averaged Green's functions [see Eqs. (57) and (58) below]. For the purpose of this section, we can ignore the boundary effects and use the bulk Green's function in the calculations. We consider the system in the presence of randomly distributed impurities with short-range potential $V_{\text{imp}}(\mathbf{r}) = u_0 \sum_i \delta(\mathbf{r} - \mathbf{r}_i)$, and calculate the self-energy in the Born

approximation²⁹. We obtain for the retarded (advanced) self-energy the expression

$$\Sigma_{\mathbf{k}\lambda,\mathbf{k}'\lambda'}(\omega \pm 0^+) \approx \frac{\mp i\pi n_i v_0^2 \rho_F}{2} \delta_{\mathbf{k}\mathbf{k}'} \delta_{\lambda\lambda'} = \frac{\mp i}{2\tau} \delta_{\mathbf{k}\mathbf{k}'} \delta_{\lambda\lambda'}, \quad (54)$$

where $\rho_F = m_H k_F^{(H)} (1 + \xi^{3/2}) / \pi^2$ is the density of states at the Fermi energy, n_i represents the density of impurities, and $\tau = 1 / (\pi n_i v_0^2 \rho_F)$ is the mean scattering time. Notice that the self-energy in the first Born approximation is momentum independent and diagonal in both momentum and helicity. We consider here the quasi-classical limit, when the mean-free paths for heavy- and light-holes are much longer than the corresponding Fermi lengths, $l_\lambda = k_F^{(\lambda)} \tau / m_\lambda \gg 2\pi / k_F^{(\lambda)}$. Using the expression (54) for the self-energy, we obtain for the disorder-averaged retarded Green's function the usual expression¹²

$$\hat{G}_{\mathbf{k}}^R(\omega) = \left[f^R(k, \omega) + \frac{5}{4} g^R(k, \omega) \right] \hat{I} - g^R(k, \omega) (\mathbf{n}_{\mathbf{k}} \hat{\mathbf{S}})^2 = f^R(k, \omega) \hat{I} + g^R(k, \omega) \mathbf{d}(\mathbf{n}_{\mathbf{k}}) \hat{\Gamma}, \quad (55)$$

where $\mathbf{n}_{\mathbf{k}} = \mathbf{k} / |\mathbf{k}|$ is the unit vector directed along the momentum, \hat{I} represents the 4×4 unit matrix, the $\hat{\mathbf{S}}$ -matrices are given in appendix A, and $\mathbf{d}(\mathbf{n}_{\mathbf{k}}) \hat{\Gamma} = d_i(\mathbf{n}_{\mathbf{k}}) \hat{\Gamma}_i$ represents the product of a five-component unit vector that depends on the direction of \mathbf{k} . In what follows we use the technique introduced by Zhang *et al.*, which involves the five generators $\hat{\Gamma}_i$ of the SO(5) Clifford algebra¹². Finally, the coefficients f^R and g^R are independent of the direction of the momentum and read

$$\begin{Bmatrix} f^R(k, \omega) \\ g^R(k, \omega) \end{Bmatrix} = \frac{1}{2} \left[\frac{1}{\omega + \mu - \frac{k^2}{2m_H} + \frac{i}{2\tau}} \pm \frac{1}{\omega + \mu - \frac{k^2}{2m_L} + \frac{i}{2\tau}} \right], \quad (56)$$

where μ is the chemical potential. Similar expressions can be obtained for the advanced Green's function with $f^A(k, \omega) = [f^R(k, \omega)]^*$ and $g^A(k, \omega) = [g^R(k, \omega)]^*$.

We are ready now to calculate the kernel of the diffusion equation,

$$\check{D} = [\hat{I} \otimes \hat{I} - \check{\Pi}]^{-1} \quad (57)$$

where \check{D} and $\check{\Pi}$ are 16×16 matrices labeled by two pairs of "spin" indices $\sigma \in \{3/2, 1/2, -1/2, -3/2\}$, and \hat{I} is the 4×4 unit matrix. The polarizability can be expressed as a convolution of two Green's functions,

$$\Pi_{\sigma_1\sigma_2,\sigma_3\sigma_4}(\omega, \mathbf{q}) = \frac{2}{\pi \rho_F \tau} \int \frac{d^3k}{(2\pi)^3} \left[\overline{G}_{\mathbf{k}+\mathbf{q}/2}^R(\omega/2) \right]_{\sigma_3\sigma_1} \left[\overline{G}_{\mathbf{k}-\mathbf{q}/2}^A(-\omega/2) \right]_{\sigma_2\sigma_4}. \quad (58)$$

Considering now the limit $\omega \ll \epsilon_F$ and $\mathbf{q} = 0$ in Eq. (58) and performing the integral over momenta we obtain

$$\check{\Pi}(\omega, 0) = \frac{1}{2} (1 + i\omega\tau) \left[\hat{I} \otimes \hat{I} + \frac{1}{5} \sum_i \hat{\Gamma}_i \otimes \hat{\Gamma}_i \right] + \mathcal{F}(\xi) (1 + i\omega\tau) \left[\hat{I} \otimes \hat{I} - \frac{1}{5} \sum_i \hat{\Gamma}_i \otimes \hat{\Gamma}_i \right], \quad (59)$$

where \hat{I} is the 4×4 unit matrix, $\hat{\Gamma}_i$ are the gamma-matrices defined in [12], and the coefficient \mathcal{F} depends on the strength of the spin-orbit coupling. Explicitly we have

$$\mathcal{F}(\xi) = \frac{1}{4(\epsilon_F \tau)^2} \frac{\xi}{1 + \xi^3/2} \frac{(1 + \sqrt{\xi})(1 + \xi) - \frac{1}{2}(1 - \sqrt{\xi})(1 - \xi)}{(1 - \xi)^2 + \frac{1}{4(\epsilon_F \tau)^2} (1 + \xi)^2}, \quad (60)$$

where $\xi = m_L / m_H = (1 - 2\gamma) / (1 + 2\gamma)$ is the light-hole to heavy-hole mass ratio and ϵ_F is the Fermi energy. Notice that $\epsilon_F \tau \gg 1$ and, consequently, the coefficient \mathcal{F} is small, $\mathcal{F} \sim \mathcal{O}(1 / (\epsilon_F \tau)^2)$, for any value of the spin-orbit coupling satisfying the inequality $\gamma \gg 1 / (4\epsilon_F \tau)$, which is always the case for physically relevant parameters. We recall that the small spin-orbit coupling limit is not physically consistent within the Luttinger model (if $\gamma \rightarrow 0$, additional bands have to be considered), although mathematically well-defined. Formally, we have $\mathcal{F}(1) = 1/2$ and we recover the standard result for systems without spin-orbit coupling. If we substitute now the expression (59) of the polarizability into Eq. (57), we obtain for the diffuson

$$\check{D}^{-1} = \left[\frac{1}{2} - \mathcal{F}(\xi) \right] \left\{ \hat{I} \otimes \hat{I} - \frac{1}{5} \sum_i \hat{\Gamma}_i \otimes \hat{\Gamma}_i \right\} - i\omega\tau \left\{ \left[\frac{1}{2} + \mathcal{F}(\xi) \right] \hat{I} \otimes \hat{I} + \left[\frac{1}{2} - \mathcal{F}(\xi) \right] \frac{1}{5} \sum_i \hat{\Gamma}_i \otimes \hat{\Gamma}_i \right\} \quad (61)$$

The final step in our evaluation is to write the diffuson in a different representation that has a more transparent physical meaning. Explicitly, we define

$$\tilde{\mathcal{D}}_{ab} = M_{\sigma_1\sigma_2}^a \mathcal{D}_{\sigma_1\sigma_2,\sigma_3\sigma_4} M_{\sigma_3\sigma_4}^b, \quad (62)$$

where $M_{\sigma_1\sigma_2}^a$ are 4×4 matrices and summation over repeating indices is implied. The M-matrices satisfy the resolution of identity $M_{\sigma_1\sigma_2}^a M_{\sigma_2'\sigma_1'}^a = \delta_{\sigma_1\sigma_1'} \delta_{\sigma_2\sigma_2'}$ and have the property $\text{Tr}[(\hat{M}^a)^2] = 1$. In particular, $M_{\sigma_1\sigma_2}^0 = \delta_{\sigma_1\sigma_2}/2$ represents the charge channel, while $\hat{M}^1 = \hat{S}_x/\sqrt{5}$, $\hat{M}^2 = \hat{S}_y\sqrt{5}$, and $\hat{M}^3 = \hat{S}_z\sqrt{5}$ correspond to the spin channels. Notice that the original quantity is a 16×16 matrix and, consequently, there will be 12 other channels, in addition to charge and spin, corresponding to higher magnetic moments.³⁰ In fact Eq. (62) can be viewed as a multipole expansion of the density matrix³⁰ with the additional channels associated with the five Γ -matrices which are quadratic combination of the spin matrices¹² (“quadrupole moments”) and seven linearly independent matrices containing cubic terms¹² (“octupole moments”). Introducing the result (61) in Eq. (62) we obtain the kernel of the diffusion equation in the new representation

$$\tilde{\mathcal{D}}_{ab}^{-1}(\omega, 0) = \left[\frac{1}{2} - \mathcal{F}(\xi) \right] \alpha_a \delta_{ab} - i\omega\tau \left[\frac{1}{2}\beta_a + \mathcal{F}(\xi)\alpha_a \right] \delta_{ab}, \quad (63)$$

with

$$\alpha_a = 1 - \frac{1}{5} \sum_i \text{Tr}[\hat{M}^a \hat{\Gamma}_i \hat{M}^a \hat{\Gamma}_i], \quad \beta_a = 1 + \frac{1}{5} \sum_i \text{Tr}[\hat{M}^a \hat{\Gamma}_i \hat{M}^a \hat{\Gamma}_i]. \quad (64)$$

Finally, from equation (63) we evaluate the relaxation times

$$\frac{1}{\tau_a} = \frac{[\frac{1}{2} - \mathcal{F}(\xi)] \alpha_a}{\frac{1}{2}\beta_a + \mathcal{F}(\xi)\alpha_a} \frac{1}{\tau} \approx \frac{\alpha_a}{\beta_a} \frac{1}{\tau}, \quad (65)$$

where for the approximation we considered physically relevant parameters satisfying $1 - \xi \gg 1/(\epsilon_F\tau)$. Formally, in the limit of vanishing spin-orbit interaction $\xi = 1$ we have $\mathcal{F}(1) = 1/2$ and all the relaxation times become infinite. However, in the physically relevant regime, relaxation is naturally absent only in the charge channel as $\alpha_0 = 0$ and $\beta_0 = 2$. The spin relaxation times are

$$\tau_x = \tau_y = \tau_z = \frac{3}{2}\tau.$$

The relaxation times for the “quadrupole” and “octupole” channels are

$$\tau_q = \frac{\tau}{4} \quad \text{and} \quad \tau_o = \frac{3}{2}\tau.$$

Notice that all these relaxation times do not depend on the spin-orbit coupling [if $1 - m_L/m_H \gg (\epsilon_F\tau)^{-1}$] and are comparable with the scattering time. Thus, these channels can not be described within the diffusion approximation.

V. CONCLUSION

We have found that the boundary spin Hall effect in a clean hole-doped semiconductor can be viewed as current-induced Friedel oscillations of the spin density with a net spin accumulation originating, in particular, from the localized surface states of the light-holes. Although, the explicit results derived in this paper are specific to the Luttinger model, the main qualitative conclusions generalize to other spin-orbit coupled systems.^{31,32} Indeed, the existence of a Fermi surface in a metal or a semiconductor inevitably leads to the Friedel oscillations if a perturbation (such as a boundary or an impurity) is introduced in the Fermi gas. In the presence of a spin-orbit coupling, there are multiple Fermi surfaces and therefore there should be Friedel oscillations with multiple periods. It is also clear that the existence of multiple Fermi surfaces should lead to the appearance of surface states: As one can see from the derivation of Sec. II, these states occur due to the impossibility to satisfy the energy and momentum conservation laws simultaneously if a majority carrier is reflected from the boundary having a large angle of incidence. This results in the appearance of localized surface states of minority carriers.^{33,34} We note that since different types of carriers appear due to the spin-orbit splitting and have different spin properties, the surface states of minority carriers will always lead to a boundary spin accumulation if there is an equilibrium charge current present. These boundary

states may also be important in the context of spin diffusion in disordered systems with weak spin-orbit coupling. Indeed, it has been shown that the boundary spin accumulation in such systems is extremely sensitive to the boundary conditions.^{35,36,37,38,39} The existence of the surface states may affect boundary conditions, since the “localization” of the minority carriers at the boundary would mimic a partially transparent interface. We note here that this effect is definitely non-perturbative and cannot be captured within expansions in powers of spin-orbit coupling, which is usually used in the context of spin diffusion.

It seems plausible that the existence of the Tamm-like surface states can be connected to the Fermi surface Berry’s phase structure in spin-orbit coupled systems, but this connection remains unclear at this stage. It is also unclear whether the spin Hall conductivity can be related to any of the observable properties in the spin Hall type experiment. In our analysis, we have not been able to identify such quantities, although the orientation of the spin accumulated near the boundary qualitatively agrees with the predictions of the spin-current theory. The main inconsistency is that the spin Hall conductivity tends to a finite constant if the spin-orbit coupling is small, while the spin accumulation calculated here depends strongly on the spin-orbit coupling γ and vanishes if the latter goes to zero.

We emphasize that our qualitative analysis is applicable only at length-scales much smaller than the mean-free path. At larger length scales different mechanisms of spin accumulation come into play. One such mechanism is due to the Dyakonov-Perel-like spin relaxation,^{40,41,42} which together with the spin-charge coupling may provide another contribution to spin accumulation. However, as shown in Sec. IV, the spin relaxation times are always too short in the framework of the Luttinger model and therefore the above-mentioned disorder-induced spin accumulation will decay exponentially at distances of order mean free-path. In particular, this implies that the semiclassical diffusion approach is not applicable to the problem.

In summary, we have constructed an exact orthonormal basis for the isotropic Luttinger model in half-space. It contains the usual incident and reflected waves as well as novel localized light-hole states. These surface states contribute to the net spin accumulation in response to a charge current. To experimentally observe the predicted surface states, it may be useful to consider a set-up in which a three-dimensional semiconductor (e.g., GaAs) exists in a close proximity to a low-dimensional system (which does not necessarily have a strong spin-orbit coupling) with a contact near the three-dimensional boundary. In this case, applying current to the system would result in spin injection into the low-dimensional system, which should be directly observable by the means of the Kerr effect. The experimental verification of the predicted spin-polarized surface states in hole-doped semiconductors is clearly called for.

Acknowledgments

The authors are grateful to Anton Burkov, Alexei Kaminski, Boris Spivak, and Maxim Vavilov for valuable insights.

APPENDIX A: SPIN 3/2 MATRICES AND SPINORS

The expressions for the S matrices in a basis with the total angular momentum parallel to the z axis are:

$$\hat{S}_x = \begin{pmatrix} & \frac{\sqrt{3}}{2} & & \\ \frac{\sqrt{3}}{2} & & 1 & \\ & 1 & & \frac{\sqrt{3}}{2} \\ & & \frac{\sqrt{3}}{2} & \end{pmatrix}, \quad \hat{S}_y = \begin{pmatrix} & -\frac{\sqrt{3}}{2}i & & \\ \frac{\sqrt{3}}{2}i & & -i & \\ & i & & -\frac{\sqrt{3}}{2}i \\ & & \frac{\sqrt{3}}{2}i & \end{pmatrix}, \quad \hat{S}_z = \begin{pmatrix} \frac{3}{2} & & & \\ & \frac{1}{2} & & \\ & & -\frac{1}{2} & \\ & & & -\frac{3}{2} \end{pmatrix}. \quad (\text{A1})$$

For a translation invariant system the eigenvectors of the Luttinger Hamiltonian are given by equation (3). The four component spinors $U_\lambda(\mathbf{n}_\mathbf{k})$ depend on the orientation, not the magnitude, of the wave vector, so each of them can be uniquely described by two angles. For the purpose of this article it is enough to know their expressions in a particular coordinate system in which the y -component of the wave vector is zero, $k_y = 0$. Consequently, the spinors will depend on one angle θ , which we choose as the angle between the z -axis and the vector $-\mathbf{k}$. Explicitly we have for $\theta < \theta_c$

$$U_{H+}(\theta) = \begin{pmatrix} \sin^3(\frac{\theta}{2}) \\ \sqrt{3} \cos(\frac{\theta}{2}) \sin^2(\frac{\theta}{2}) \\ \sqrt{3} \cos^2(\frac{\theta}{2}) \sin(\frac{\theta}{2}) \\ \cos^3(\frac{\theta}{2}) \end{pmatrix}, \quad U_{L+}(\theta) = \begin{pmatrix} -\sqrt{3} \cos(\frac{\theta}{2}) \sin^2(\frac{\theta}{2}) \\ -1/2 [1 + 3 \cos(\theta)] \sin(\frac{\theta}{2}) \\ 1/2 [1 - 3 \cos(\theta)] \cos(\frac{\theta}{2}) \\ \sqrt{3} \cos^2(\frac{\theta}{2}) \sin(\frac{\theta}{2}) \end{pmatrix},$$

$$U_{H-}(\theta) = U_{H+}(\pi + \theta), \quad U_{L-}(\theta) = U_{L+}(\pi + \theta). \quad (\text{A2})$$

For an incident angle $\theta > \theta_c$ there are no light-holes propagating in the z direction, but localized solutions described by the spinors

$$\begin{aligned}
 V_1(\chi) &= \frac{1}{2\sqrt{2} [1 + \sin(\chi) + \sin^2(\chi)]} \begin{pmatrix} i\sqrt{3} \\ 1 + 2\sin(\chi) \\ -i[1 + 2\sin(\chi)] \\ -\sqrt{3} \end{pmatrix}, \\
 V_2(\chi) &= \frac{1}{2\sqrt{2} [1 - \sin(\chi) + \sin^2(\chi)]} \begin{pmatrix} -\sqrt{3} \\ -i[1 - 2\sin(\chi)] \\ 1 - 2\sin(\chi) \\ i\sqrt{3} \end{pmatrix}.
 \end{aligned} \tag{A3}$$

APPENDIX B: SCATTERING COEFFICIENTS FOR AN INCIDENT HEAVY-HOLE WITH HELICITY $+3/2$

The scattering coefficients A_i and B_i in Eq. (5) are functions of the incident angle θ and can be obtained by imposing the boundary condition $\psi_{\mathbf{k}}^{(H+)}(z=0) = 0$. Explicitly we have

$$\begin{pmatrix} A_1(\theta) \\ A_2(\theta) \\ B_1(\theta) \\ B_2(\theta) \end{pmatrix} = \frac{1}{5 + 3\cos[2(\phi(\theta) - \theta)]} \begin{pmatrix} -(4 - 3\cos[2\phi(\theta)] - \cos[2\theta])\sin[\theta] \\ (4 + 3\cos[2\phi(\theta)] + \cos[2\theta])\cos[\theta] \\ \sqrt{3}(\sin[\frac{1}{2}(\phi(\theta) - 3\theta)] - 3\sin[\frac{1}{2}(3\phi(\theta) - \theta)])\sin[2\theta] \\ \sqrt{3}(\cos[\frac{1}{2}(\phi(\theta) - 3\theta)] + 3\cos[\frac{1}{2}(3\phi(\theta) - \theta)])\sin[2\theta] \end{pmatrix}, \tag{B1}$$

where $\phi(\theta)$ characterizes the light-hole wave and is given by Eq. (7).

In the presence of the localized modes, by imposing the boundary condition, $\psi_{\mathbf{k}}^{(H+)}(z=0) = 0$ we obtain for the scattering coefficients in Eq. (9)

$$\begin{pmatrix} A_1(\theta) \\ A_2(\theta) \\ B_1(\theta) \\ B_2(\theta) \end{pmatrix} = \begin{pmatrix} \frac{[-13 + \cos(2\theta) - \cos(2\chi) + \cos(2\theta)\cos(2\chi)]\sin(\theta)}{5 + 9\cos(2\theta) + 5\cos(2\chi) + 3\cos(2\theta)\cos(2\chi) + 12i\sin(2\theta)\sin(\chi)} \\ \frac{[-5 + \cos(2\theta) + 7\cos(2\chi) + \cos(2\theta)\cos(2\chi)]\cos(\theta)}{5 + 9\cos(2\theta) + 5\cos(2\chi) + 3\cos(2\theta)\cos(2\chi) + 12i\sin(2\theta)\sin(\chi)} \\ \frac{-i\sqrt{3}\sqrt{3 - \cos(2\chi) + 2\sin(\chi)}[\cos(\frac{\theta}{2}) - i\sin(\frac{\theta}{2})]\sin(\theta)}{2\cos(\theta)(1 + 2\sin(\chi)) - 2i\sin(\theta)(2 + \sin(\chi))} \\ \frac{-\sqrt{3}\sqrt{3 - \cos(2\chi) - 2\sin(\chi)}[\cos(\frac{\theta}{2}) + i\sin(\frac{\theta}{2})]\sin(\theta)}{2\cos(\theta)(1 - 2\sin(\chi)) + 2i\sin(\theta)(2 - \sin(\chi))} \end{pmatrix}. \tag{B2}$$

- ¹ J. M. Luttinger, Phys. Rev. **102**, 1030 (1956).
- ² S. Murakami, N. Nagaosa, and S.-C. Zhang, Science **301**, 1348(2003).
- ³ J. Sinova, D. Culcer, Q. Niu, N. A. Sinitsyn, T. Jungwirth, and A. H. MacDonald, Phys. Rev. Lett. **92**, 126603 (2004).
- ⁴ S. A. Wolf, D. D. Awschalom, R. A. B. J. M. Daughton, S. von Molnar, M. L. Roukes, A. Y. Chtchelkanova, and D. M. Treger, Science **294**, 1488-1495 (2001).
- ⁵ I. Zutic, J. Fabian, and S. Das Sarma, Rev. Mod. Phys. **76**, 323-410 (2004).
- ⁶ Y. K. Kato, R. Myers, A. Gossard, and D. Awschalom, Science **306**, 1910 (2004).
- ⁷ V. Sih, R. C. Myers, Y. K. Kato, W. H. Lau, A. C. Gossard, and D. D. Awschalom, Nature Phys. **1**, 31 (2005).
- ⁸ J. Wunderlich, B. Kaestner, J. Sinova, and T. Jungwirth, Phys. Rev. Lett. **94**, 047204 (2005).
- ⁹ J. Sinova, S. Murakami, S.-Q. Shen, and M.-S. Choi, <http://arxiv.org/cond-mat/0512054> (2005).
- ¹⁰ S. Zhang, Phys. Rev. Lett. **85**, 393 (2000).
- ¹¹ G. Sundaram and Q. Niu, Phys. Rev. B **59**, 14915-14925 (1999).
- ¹² S. Murakami, N. Nagaosa, and S. C. Zhang, Phys. Rev. B **69**, 235206 (2004).
- ¹³ F. D. M. Haldane, Phys. Rev. Lett. **93**, 206602 (2004).
- ¹⁴ H.-A. Engel, B. I. Halperin, and E. I. Rashba, Phys. Rev. Lett. **95**, 166605 (2005).
- ¹⁵ W.-K. Tse and S. Das Sarma, Phys. Rev. Lett. **96**, 056601 (2006).
- ¹⁶ B. A. Bernevig, T. L. Hughes, and S.-C. Zhang, Phys. Rev. Lett. **95**, 066601 (2005).

- ¹⁷ B. A. Bernevig and S.-C. Zhang, Phys. Rev. Lett. **95**, 016801 (2005).
- ¹⁸ J. Schliemann and D. Loss, Phys. Rev. B **71**, 085308 (2005).
- ¹⁹ B. A. Bernevig and S. C. Zhang, Phys. Rev. Lett. **95**, 016801 (2005).
- ²⁰ J. Shi, P. Zhang, D. Xiao, and Q. Niu, Phys. Rev. Lett. **96**, 076604 (2006).
- ²¹ E. I. Rashba, Phys. Rev. B **68**, 241315 (2003).
- ²² I. E. Tamm, Z. Phys. **76**, 849 (1932).
- ²³ P. G. de Gennes, J. Phys. Radium **23**, 630 (1962).
- ²⁴ A. Y. Zyuzin and B. Z. Spivak, Pisma Zh. Eksp. Teor. Fiz. **43**, 185 (1986) [JETP Lett. **43**, 234 (1986)].
- ²⁵ I. V. Lerner, Phys. Rev. B **48**, 9462 (1993).
- ²⁶ V. M. Galitski, M. G. Vavilov, and L. I. Glazman, Phys. Rev. Lett. **94**, 096602 (2005).
- ²⁷ A. A. Burkov, A. S. Núñez, and A. H. MacDonald, Phys. Rev. B **70**, 155308 (2004).
- ²⁸ E. G. Mishchenko, A. V. Shytov, and B. I. Halperin, Phys. Rev. Lett. **93**, 226602 (2004).
- ²⁹ S. Murakami, Phys. Rev. B **69**, 241202(R) (2004).
- ³⁰ R. Winkler, Phys. Rev. B **70**, 125301 (2004).
- ³¹ E. I. Rashba, Sov. Phys. Solid State **2**, 1224-1238 (1960) [Fiz. Tverd. Tela (Leningrad) **2**, 1109-1122 (1960)].
- ³² G. Dresselhaus, Phys. Rev. **100**, 580-586 (1955).
- ³³ G. Usaj and C. A. Balseiro, Europhys. Lett. **72**, 631 (2005).
- ³⁴ A. Shekhter, M. Khodas, and A. M. Finkelstein, Phys. Rev. B **71**, 125114 (2005).
- ³⁵ V. Sih, W. H. Lau, R. C. Myers, V. R. Horowitz, A. C. Gossard, and D. Awschalom, cond-mat/0605672 (2006).
- ³⁶ W.-K. Tse, J. Fabian, I. Zutic, and S. Das Sarma, Phys. Rev. B **72**, 241303 (2005).
- ³⁷ V. M. Galitski, A. A. Burkov, and S. Das Sarma, <http://arxiv.org/cond-mat/0601677> (2006).
- ³⁸ A. G. Malshukov, L. Y. Wang, C. S. Chu, and K. A. Chao, Phys. Rev. Lett. **95**, 146601 (2005).
- ³⁹ I. Adagideli and G. E. W. Bauer, Phys. Rev. Lett. **95**, 256602 (2005).
- ⁴⁰ M. I. Dyakonov and V. I. Perel, Phys. Lett. **35A**, 459 (1971).
- ⁴¹ M. I. Dyakonov and V. I. Perel, JETP Lett. **13**, 467 (1971).
- ⁴² V. M. Edelstein, Solid State Commun., **73**, 233 (1990).